Induction of MET by Ionizing Radiation and Its Role in Radioresistance and Invasive Growth of Cancer

Induction of MET by Ionizing Radiation and Its Role in Radioresistance and Invasive Growth of Cancer

Francesca De Bacco, Paolo Luraghi, Enzo Medico, Gigliola Reato, Flavia Girolami,Timothy Perera, Pietro Gabriele, Paolo M. Comoglio and Carla Boccaccio

Affiliations of authors: IRCC—Institute for Cancer Research at Candiolo, University of Turin Medical School, Candiolo, Italy (FDB, PL, EM, GR, FG, PG, PMC, CB); Janssen Research & Development—Janssen Pharmaceutica NV, Turnhoutseweg, Beerse, Belgium (TP)

Correspondence to: Carla Boccaccio, MD (carla.boccaccio@ircc.it) and Paolo M. Comoglio, MD (e-mail: pcomoglio@gmail.com), IRCC—Institute for Cancer Research at Candiolo, University of Turin Medical School, Strada Provinciale 142, Candiolo 10060, Italy.

Abstract

Background Ionizing radiation (IR) is effectively used in cancer therapy. However, in subsets of patients, a few radioresistant cancer cells survive and cause disease relapse with metastatic progression. The *MET*oncogene encodes the hepatocyte growth factor (HGF) receptor and is known to drive “invasive growth”, a regenerative and prosurvival program unduly activated in metastasis.

Methods Human tumor cell lines (MDA-MB-231, MDA-MB-435S, U251) were subjected to therapeutic doses of IR. MET mRNA, and protein expression and signal transduction were compared in treated and untreated cells, and the involvement of the DNA-damage sensor ataxia telangiectasia mutated (ATM) and the transcription factor nuclear factor kappa B (NF-ºB) in activating MET transcription were analyzed by immunoblotting, chromatin immunoprecipitation, and use of NF-ºB silencing RNA (siRNA). Cell invasiveness was measured in wound healing and transwell assays, and cell survival was measured in viability and clonogenic assays. MET was inhibited by siRNA or small-molecule kinase inhibitors (PHA665752 or JNJ-38877605). Combinations of MET-targeted therapy and radiotherapy were assessed in MDA-MB-231 and U251 xenografts (n = 5–6 mice per group). All *P* values were from two-sided tests.

Results After irradiation, MET expression in cell lines was increased up to fivefold via activation of ATM and NF-ºB. MET overexpression increased ligand-independent MET phosphorylation and signal transduction, and rendered cells more sensitive to HGF. Irradiated cells became more invasive via a MET-dependent mechanism that was further enhanced in the presence of HGF. MET silencing by siRNA or inhibition of its kinase activity by treatment with PHA665752 or JNJ-38877605 counteracted radiation-induced invasiveness, promoted apoptosis, and prevented cells from resuming proliferation after irradiation in vitro. Treatment with MET inhibitors enhanced the efficacy of IR to stop the growth of or to induce the regression of xenografts (eg, at day 13, U251 xenografts, mean volume increase relative to mean tumor volume at day 0: vehicle = 438%, 5Gy IR = 151%, 5 Gy IR + JNJ-38877605 = 76%; difference, IR vs JNJ-38877604 + IR = 75%, 95% CI = 59% to 91%, *P* = .01).

Conclusion IR induces overexpression and activity of the MET oncogene through the ATM-NF-ºB signaling pathway; MET, in turn, promotes cell invasion and protects cells from apoptosis, thus supporting radioresistance. Drugs targeting MET increase tumor cell radiosensitivity and prevent radiation-induced invasiveness.

Radiotherapy can be used successfully for local treatment of primary cancer (1). However, a fraction of tumors recur after this treatment and are usually more aggressive [(2) and references therein]. Consistent with these clinical observations, pioneering work by Kaplan and Murphy (3), studies in classical animal models [(4) and references therein], and in vitro experiments (5,6) have shown that ionizing radiation (IR) can exert a paradoxical prometastatic effect. This effect is observed after radiation doses that are insufficient to eradicate the primary tumor and seldom after curative radiation treatment. More recent experiments have indicated that IR promotes positive selection of a preexisting, intrinsically radioresistant "cancer stem cell" subpopulation, offering an attractive mechanistic explanation for radiation-induced tumor progression (7–9). However, there is also striking evidence that, in some cells, IR induces an adaptive phenotype aimed at tissue regeneration that can result in metastatic behavior (10). This phenotype, which has been referred to as the "stress-and-recovery" response to DNA damage (10), occurs both at the single cell and tissue levels. In single cells, DNA damage detection elicits specific molecular mechanisms, mostly orchestrated by the ataxia telangiectasia mutated (ATM)-p53 axis, that blocks replication and activate DNA repair (11). If repair fails, a normal cell is programmed to execute apoptosis or to undergo proliferative arrest through senescence. Nevertheless, after the death of radiation-damaged cells, tissues must restore their adequate cell number, pattern, and function via regeneration (or "wound healing") by the surviving cells, either normal or neoplastic. As observed in vitro, this process includes detachment from the wound border, acquisition of a fibroblast phenotype, migration into the empty area, and, possibly, proliferation. This complex program has been referred to as "epithelial-mesenchymal transition" [EMT; (12)], and, more recently also as "invasive growth" [IG; (13,14)], to emphasize its functional relevance for cancer. It is now widely accepted that EMT or IG is a physiological program for tissue development and regeneration that is inappropriately activated in cancer cells, often as an adaptive response to adverse environmental conditions, thus leading to invasion and metastasis (14–16).

The EMT or IG genetic program is ultimately controlled by a few specific transcription factors and extracellular signals (17). The latter group includes scatter factors, such as hepatocyte growth factor (HGF) and macrophage stimulating protein (MSP), which activate tyrosine kinase receptors belonging to the HGF receptor (MET) oncogene family (13).

An association between IR-induced cell invasion and MET expression has been suggested for neuroblastoma and pancreatic cancer cells, but a causal relationship was never established (18,19). Here we investigated 1) whether MET expression and signaling were increased in response to IR in a panel of human cancer cells, and by what mechanism; 2) whether MET expression and activity are required for IR-induced cell invasion; and 3) whether specific MET kinase inhibitors can prevent IR-induced cell invasion and sensitize cancer cells to radiotherapy in vitro and in vivo.

Methods

Cell Lines, Compounds, and Silencing RNA (siRNA)

Human cell lines (breast carcinomas MDA-MB-231 and MDA-MB-435S; glioma U251, U-87MG and SF295; lung carcinoma A549; colon carcinomas LoVo and DLD1; prostate carcinoma PC3; neuroblastoma SK-N-SH; and normal fibroblast MRC-5) were purchased from ATCC (Rockville, MD), kept in culture for less than 8 weeks, and used between passages 2 and 20 (the identity of MDA-MB-435S is controversial and has recently been defined as melanoma:http://dtp.nci.nih.gov/docs/misc/common_files/mda-mb-435-update.html). Following the provider's instructions, cells were cultured in Dulbecco's modified Eagle medium (DMEM)-high glucose or RPMI-1640 (Sigma, St Louis, MO) supplemented with 10% fetal bovine serum (Lonza Sales Ltd, Basel, Switzerland) and 2 mM glutamine (Sigma) in a humidified atmosphere with 5%

CO_2 at 37°C. For experiments requiring hypoxic conditions (1% O_2), cells were cultured in a Heraeus BB 6220 oxygen electrode incubator (Hereaus, Hanau, Germany). For activation of MET signaling, recombinant human HGF (50 ng/mL; R&D Systems, Minneapolis, MN) was added to the culture medium. For MET kinase inhibition, cells were treated with PHA665752 (500 nM; Tocris Cookson Ltd, Bristol, UK) dissolved in dimethyl sulfoxide (DMSO; Sigma) immediately before irradiation, and were kept in the presence of the inhibitor. The MET kinase inhibitor JNJ-38877605 was produced by Janssen Research & Development (Janssen Pharmaceutica NV, Beerse, Belgium). siRNAs targeting MET or RELA (nuclear factor kappa B [NF-ºB]) mRNA, or control siRNAs (ON-TARGET plus SMART pool; Dharmacon, Lafayette, CO) were transiently transfected into MDA-MB-231, MDA-MB-435S, or U251 cells (final concentration: 100 nM per each 30%–50% confluent cell plate) using Lipofectamine 2000 (Invitrogen, Carlsbad, CA) according to manufacturer's instructions. For inhibition of the ATM kinase, cells were pretreated with CGK733 (10 µM in DMSO; Sigma) for 4 hours before irradiation and then kept in the presence of the inhibitor.

Irradiation

Cells (MDA-MB-231, MDA-MB-435S, or U251) or mice were exposed to conventional X-rays (1–10 Gy, 3 Gy per minute) emitted by a linear particle accelerator used for human radiotherapy (Clinac 600C/D; Varian, Palo Alto, CA) operated at 6 MV and at room temperature.

Immunoblots

Protein expression, phosphorylation, and nuclear translocation in irradiated MDA-MB-231, MDA-MB-435S, or U251 cells were evaluated by immunoblotting. To minimize the stimulatory effects of growth factors on MET transcription, confluent cells were serum starved for 48 hours and then irradiated. To obtain whole-cell lysates, 2–4 × 10^6 cells were solubilized in boiling Laemmli buffer (100 µL per 10^6 cells). For analysis of mitogen-associated protein (MAP) kinase phosphorylation, cells were lysed in RIPA buffer [20 mM Tris–HCl pH 6.8, 150 mM NaCl, 1% TRITON X-100, 5 mM EDTA, 1% Na-deoxycholate, 0.5% sodium dodecyl sulfate (SDS), 1 mM Na_3VO_4, 1 mM phenylmethylsulfonyl fluoride, and a cocktail of protease inhibitors]. To fractionate cytoplasmic and nuclear proteins, cells were washed and incubated on ice for 10 minutes in “buffer A” (10 mM HEPES pH 7.9, 10 mM KCl, 0.1 mM EDTA, 0.5% NP-40, 1 mM dithiothreitol, 1 mM phenylmethylsulfonyl fluoride, and a cocktail of protease inhibitors). Supernatants, containing the cytoplasmic extracts, were separated by centrifugation (9600*g*, 5 minutes). Pellets were resuspended in “buffer B” (20 mM HEPES pH 7.9, 400 mM KCl, 1 mM EDTA, 1 mM dithiothreitol, 10% glycerol, 1 mM phenylmethylsulfonyl fluoride, and a cocktail of protease inhibitors) and incubated at 4°C for 1 hour with vigorous mixing. The resulting nuclear lysates were clarified by high-speed centrifugation. Protein concentration was determined using a BCA Protein Assay Reagent kit (Pierce Biotechnology, Rockford, IL). Equal amounts of proteins were resolved by SDS polyacrylamide gel electrophoresis in reducing conditions and analyzed by immunoblotting with the following antibodies: mouse monoclonal anti-MET (DL21, 1:1500) (20), rabbit polyclonal anti-phospho-p42/44 MAP kinase (1:1000; Cell Signaling Technology, Danvers, MA), rabbit polyclonal anti-p42/44 MAP kinase (1:1000; Cell Signaling Technology), mouse monoclonal anti-p65/RelA (1:500; BD Biosciences, Bredford, MA), mouse anti-hypoxia inducible factor-1 (anti-HIF-1±) (1:350; BD Biosciences), rabbit polyclonal anti-phosphoserine 276 (1:1000; Cell Signaling Technology), rabbit polyclonal anti-caspase-3 (1:1000; Cell Signaling Technology), rabbit polyclonal anti-phospho-Chk2 (1:2000, T68; R&D Systems Minneapolis, MN), goat polyclonal anti-actin (1:3000, C-11; Santa Cruz Biotechnology, Santa Cruz, CA), and mouse monoclonal anti-lamin B (5µg/mL; Calbiochem, Darmstadt, Germany). For analysis of MET phosphorylation, cells were lysed in radioimmunoprecipitation assay (RIPA) buffer. Equal amounts of proteins were immunoprecipitated

using mouse monoclonal anti-MET antibodies (DQ13) (21), and analyzed by immunoblotting with mouse monoclonal anti-phosphotyrosine antibodies (1:1000; UBI, Lake Placid, NY). The same blots were stripped with a solution containing 62.5 mM Tris–HCl pH 6.8, 2% SDS, and 100 mM 2-mercaptoethanol at 50°C, and reprobed with anti-MET antibodies as above or rabbit polyclonal anti-Gab1 antibodies (1:1000; Millipore, Temecula, CA). Antibodies were visualized with appropriate horseradish peroxidase–conjugated secondary antibodies (Amersham, Uppsala, Sweden), and the enhanced chemiluminescence system (Amersham). For control of equal amount of protein loading, blots were stripped as above and/or reprobed with anti-actin antibodies, or with anti-lamin B antibodies. Blot images were captured using a molecular imager (GelDoc XR; Bio-Rad Laboratories, Hercules, CA). Densitometric analysis was performed with Quantity One 1-D (Bio-Rad Laboratories). Immunoblots shown are representative of results obtained in at least three independent experiments.

Northern Blot

Northern blots were used to evaluate MET transcriptional induction by IR. Confluent MDA-MB-231, MDA-MB-435S, and U251 cells were serum starved for 48 hours and irradiated (10 Gy). Total RNA was isolated using the RNeasy Mini Kit (Qiagen, GmbH, Hilden, Germany) according to manufacturer's instructions. Equal amounts (15 µg) of purified RNA were resolved on 0.8% agarose-formaldehyde gels and transferred to Hybond-N nylon membranes (Amersham). The MET probe containing the complete coding sequence (GenBank accession number J02958) was obtained from the pCEV-MET plasmid (22) and labeled with a random priming kit (Megaprime; Amersham) using [±-^{32}P]-dCTP. Hybridization was carried out at 42°C for 16 hours in the presence of 50% formamide. Nylon membranes were washed twice with 2× saline-sodium citrate (SSC)–0.1% SDS and twice with 0.1× SSC–0.1% SDS at 42°C and then autoradiographed. Northern blots shown are representative of results obtained in at least two independent experiments.

Luciferase Reporter Assay

Luciferase reporter assays were used to evaluate the activity of the *MET* promoter in irradiated MDA-MB-231 and MDA-MB-435S cells. The construct pGL2-3.1, which encodes the luciferase gene under control of the human full-length *MET* promoter sequence (GenBank accession number AF046925), has previously been described (23). The promoterless pGL2-basic plasmid encoding luciferase (Promega, Madison, WI) was used as control. Cells were seeded in 24-well plates and grown to confluence. Transient transfections were performed using Lipofectamine 2000 (Invitrogen) following the manufacturer's protocol. Transfected cells were serum starved for 24 hours and subsequently irradiated (10 Gy). When indicated, cells were transfected with siRNAs 24 hours before the promoter plasmids were introduced. Luciferase activity was measured on a GloMax 96-well microplate luminometer (Promega) using the Promega Luciferase Reporter Assay System according to manufacturer's instructions. Protein concentrations were determined with Protein Assay Dye Reagent (Bio-Rad) and used to normalize luciferase activity. The reported luciferase activities are the mean values from at least six samples from at least two independent experiments.

Endpoint and Quantitative Real-Time–Polymerase Chain Reaction (RT-PCR)

Transcription of cytokines and growth factors in irradiated MDA-MB-231, MDA-MB435S, U251, and MRC-5 cells was evaluated by PCR. Total RNA was purified from irradiated cells as described above. Two micrograms of RNA was used as a template for cDNA synthesis with random hexamer primers and the High Capacity Reverse Transcription kit (Applied Biosystems, Foster City, CA) according to manufacturer's instructions. Endpoint PCR was performed using the following primers: HGF [sense, 5′-TTTCACCCAGGCATCTCCTCCAGAG-3′; antisense, 5′-

CGTAGGTCCTTGCACTTGAAA-3′, and GAPDH [sense, 5′-accacagtccatgccatcac-3′; antisense, 5′-tccaccaccctgttgctgta-3′]. PCR conditions were as follows: 95°C, 30 seconds; 58°C, 30 seconds; 72°C, 1 minute; 35 cycles. RT-PCR was performed using commercially available primer and probe sets for HGF, tumor necrosis factor-α (TNF-α), interleukin 6, MSP, and transforming growth factor-β (TGF-β) (Applied Biosystems), with TaqMan PCR Master Mix (Applied Biosystems) on an ABI PRISM 7900HT sequence detection system (Applied Biosystems). Relative quantification values for target genes were obtained by normalizing against an endogenous control (β-actin) and a calibrator (nonirradiated cells). Two repetitions of the experiment were performed using independently prepared cDNA. All samples were analyzed in triplicate.

Chromatin Immunoprecipitation (ChIP)

ChIP was used to investigate binding of transcription factor NF-κB to the endogenous *MET* promoter in irradiated MDA-MB-231 cells. We used 4×10^7 cells for 10 immunoprecipitations either from irradiated or control cells. Nuclei were pelleted, resuspended in 1 mL of SDS lysis buffer (1% SDS, 1 mM EDTA, 50 mM Tris–HCl pH 8, and a cocktail of protease inhibitors), and disrupted by sonication, yielding DNA fragments with a bulk size of 400–1000 bp. Chromatin preparations were diluted, and precleared with protein G-Sepharose (Amersham). Three percent of each chromatin preparation 3% of chromatin preparation was used as the input for ChIP normalization. ChIP was performed overnight at 4°C with 4 μg of antibodies (rabbit polyclonal anti-p65/RelA, Santa Cruz Biotechnology; total mouse immunoglobulin G [IgG], Millipore), followed by incubation with 50 μL of protein G-Sepharose beads for 3 hours. ChIPs were washed, eluted twice in elution buffer (1% SDS, 0.1 M $NaHCO_3$), and kept overnight at 65°C to reverse formaldehyde cross-linking. Samples were treated with RNase (50 μg/mL, 37°C for 30 minutes) and Proteinase-K (500 μg/mL, 45°C for 2 hours). Each sample was purified and used as template for RT-PCR using SYBR GREEN PCR Master Mix (Applied Biosystems) and the following primers: NFKBIA [sense, 5′-GAACCCCAGCTCAGGGTTTAG-3′; antisense, 5′-GGGAATTTCCAAGCCAGTCA-3′], κB1 (MET) [sense, 5′-AGGCCCAGTGCCTTATTACCA-3′; antisense, 5′-GCGGCCTGACTGGAGATTT-3′], and –κB1 (MET) [sense, 5′-GGGACTCAGTTTCTTTACCTGCAA-3′; antisense, 5′-GGGACTCAGTTTCTTTACCTGCAA-3′] (further details can be found in Supplementary Materials and Methods).

Reactive Oxygen Species (ROS) Detection

To evaluate ROS production in irradiated MDA-MB-231, MDA-MB-435S, and U251 cells, we measured ROS-mediated fluorescent activation of the compound 5-(and 6)-carboxy-2′,7′-dichlorofluorescein diacetate (carboxy-H_2DCFDA; Molecular Probes, Invitrogen) according to manufacturer's instructions. Briefly, cells were seeded in black 96-well plates (3×10^4 cells per well) 24 hours before irradiation. Cells were supplied with carboxy-H_2DCFDA (10 μM) in phenol red–free DMEM for 1 hour, then washed and incubated for 30 minutes in phenol red–free DMEM without carboxy-H_2DCFDA, and then irradiated (10 Gy). Treatment with H_2O_2 (100 μM) was used as positive control in nonirradiated cells. ROS generation was measured 15 minutes after irradiation using a fluorescence plate reader (λ_{ex} = 485 nm, λ_{em} = 535 nm) (DTX 880 Multimode Detector; Beckman-Coulter, Brea, CA).

Enzyme-linked Immunosorbent Assay (ELISA)

ELISAs were used to evaluate TNF-α secretion in the culture medium of irradiated MDA-MB-231 and MDA-MB-435S cells. Cells were seeded into six-well plates, grown to confluence, and serum starved for 48 hours. The culture medium was then discarded and replaced with fresh medium (1 mL) before IR treatment (10 Gy). Supernatants were removed at the indicated time points and kept at −20°C before use. ELISA was performed using a quantitative sandwich enzyme immunoassay

from R&D Systems (TNF± Quanti-Glo Chemiluminescent ELISA; R&D Systems, Minneapolis, MN) according to manufacturer's instructions. The reported measurements are the mean of six replicates from two independent experiments.

Wound Healing Assay

Wound healing assays were used to evaluate cell motility induced by irradiation. MDA-MB-231, MDA-MB-435S, and U251 cells were grown to confluence in 24-well plates, starved for 24 hours, and scraped with a P1000 pipet tip (Gilson, Inc, Middleton, WI) to make a 300−400 μM wide scratch. Culture medium was replaced with fresh medium containing 1% fetal bovine serum (FBS) supplemented with the MET inhibitor, PHA665752 (500 nM dissolved in DMSO) or with an equal volume of DMSO alone, and then immediately irradiated. After 24 hours, cells were fixed with 11% glutaraldehyde (Sigma), and stained with 0.1% crystal violet. Images were acquired with a Leica photocamera (DFC320; Leica, Wetzlar, Germany) connected with an inverted light microscope (DM IRB; Leica). Images are representative of the results obtained in at least three independent experiments.

Invasion Assay

Cell invasion induced by irradiation was measured in Transwell chambers containing 6.4 mm diameter polyethylene terphthalate filters with 8.0 μm pore size (BD Falcon, Bredford, MA). MDA-MB-231 or MDA-MB-435S cells (5×10^5 per transwell) were seeded on filters coated with 20 $\mu g/cm^2$ of reconstituted Matrigel basement membrane (BD Biosciences). U251 cells (10^4 per transwell) were seeded on filters coated with 50 $\mu g/cm^2$ of Matrigel. Culture medium supplemented with 1% FBS was added to both chambers to measure invasion due to receptor overexpression and activation (resulting from IR induction) in the absence of a chemoattractant. One hour after seeding, cells were irradiated (10 Gy) and incubated at 37°C for 24 hours. Then, cells on the upper side of the filter were mechanically removed, and those that had migrated onto the lower side of the filter were fixed, stained, and photographed as above. In some experiments, PHA665752 (500 nM), or the vehicle (DMSO), was added to both transwell chambers immediately before irradiation. Where indicated, HGF (50 ng/mL) was added to the lower chamber immediately before irradiation. For quantification of cell invasion, 10 fields per experimental condition were randomly selected and micrographed as above with a ×10 objective. Morphometric analysis was performed using MetaMorph 7.1 software (Molecular Devices, Sunnyvale, CA). Images are representative of at least three independent experiments.

Branching Morphogenesis Assay

A branching assay was used to evaluate the effect of irradiation on HGF-induced morphogenesis. MDA-MB-435S cell spheroids were preformed by resuspension of single cells in 240 mg/mL methylcellulose (Sigma) and culture in nonadherent 96-well plates (Greiner, Frickenhausen, Germany) for 24 hours. Spheroids were transferred into a matrix containing 1.3 mg/mL type I collagen from rat tail (BD Biosciences), 10% FBS, and 240 mg/mL methylcellulose. After 24 hours, cells were irradiated and/or cultured for 7 days in the presence of 50 ng/mL HGF (which had been purified as a recombinant protein from conditioned medium from baculovirus-infected SF9 insect cells). The conditioned medium from uninfected cells was used as negative (mock) control. Images are representative of results obtained in at least three independent experiments.

Cell Viability Assay

A commercial assay was used to evaluate viability of irradiated MDA-MB-231, MDA-MB-435S, and U251 cells. Cells were seeded in 96-well plates, grown to confluence, and serum starved for 24 hours. The culture medium was replaced with a medium containing 1% FBS and PHA665752 (500

nM) or the vehicle alone (DMSO), and cells were irradiated (10 Gy). Cell viability was assessed with the ATPlite one-step Luminescence Assay System kit (Perkin Elmer, Shelton, CT) according to manufacturer's instructions, using a GloMax 96 Microplate Luminometer (Promega). The reported measurements are the mean of nine replicates from three independent experiments.

Clonogenic Assay

The assay described by Franken et al. (24) was used to evaluate the clonogenic (proliferative) ability of irradiated MDA-MB-231 and U251 cells. Briefly, 25 cells per well were seeded in 24-well plates. After 16 hours, cells were irradiated (1–5 Gy) in the presence of 10% FBS and PHA665752 (500 nM) or the vehicle alone (DMSO), and cultured for 15 days. Colonies containing 50 cells or more were considered representative of clonogenic cells. The clonogenic fraction was calculated using the formula: [(number of colonies formed after treatment)/(number of cells seeded × plating efficiency)] × 100, where plating efficiency is the percentage of seeded cells that gave rise to clones under control conditions (ie, no irradiation, culture in 10% FBS without PHA665752). The reported values are the mean of eight replicates from two independent experiments.

In Vivo Cell Transplantation and Therapy

MDA-MB-231 or U251 cells were transplanted into mice to study the tumor response to radiotherapy in association with MET inhibitors. Mice were kept and manipulated under pathogen-free conditions, according to protocols approved by the Italian Ministry of Health and by the internal Ethical Committee for Animal Experimentation (FPRC-CESA). U251 cells (10^6 cells per mouse) were subcutaneously injected into the right flanks of 6-week-old female Crl:CD1-Foxn1^{nu} mice (CD1-nu$^{-/-}$, n = 24; Charles River Laboratories, Calco, Italy). MDA-MB-231 cells (10^6 cells per mouse) were resuspended in 20% Matrigel and similarly injected into 6-week old female NOD.CB17-Prkdc^{scid}/J mice (NOD/SCID, n = 20; Charles River Laboratories). After the development of tumors that were approximately 50 mm^3 in size (ie, 2–3 weeks after the cells were injected), the mice were subjected to total body irradiation. CD1-nu$^{-/-}$ mice with U251 tumors received a single dose of 5 Gy on day 0, whereas NOD/SCID mice with MDA-MB-231 tumors received a 4.5 Gy total dose that was fractionated in three 1.5 Gy doses on days 0, 2, and 4. Irradiation was preceded (on day minus 1 for U251 xenografts, on day 0 for MDA-MB-231 xenografts) and followed by daily administration of the MET inhibitor, JNJ-38877605 (50 mg/kg), by oral gavage, until the end of the experiments (day 7 for MDA-MB-231 xenografts or day 13 for U251 xenografts). Tumor diameters were measured every 3 days with a caliper and tumor volume was calculated using the formula: 4/3À × (d/2)^2 × (D/2), where d and D are the minor and the major tumor axis, respectively. Tumor volume was reported as relative volume increase with respect to mean tumor volume at time 0. The general physical status of mice was monitored daily. Mice were killed by anesthesia (zoletil 40 mg/kg + xylazine 7.5 mg/kg) followed by carbon dioxide inhalation, when they showed signs of systemic suffering (cachexia or anemia, occurring in the irradiated NOD/SCID strain), or when the tumor size exceeded 2000 mm^3. The evaluated statistical power for the reported experiments is 90%, considering the size of experimental groups, at least a twofold difference in tumor volume between experimental groups, tumor volume variation of up to 50% within groups, and a statistical significance level of ± = .05.

Histopathologic Analysis and TUNEL Assays

Terminal deoxynucleotidyl transferase dUTP nick end labeling (TUNEL) assays were used to evaluate the apoptotic index in sections of the tumors that were formed by MDA-MB-231 cells in NOD/SCID mice (see above). Mice (n = 36) were treated with a single irradiation dose (5 Gy) and/or daily administration of JNJ-38877605 through oral gavage, and were killed at days 2, 4, or 6 after irradiation. Tumors were excised, embedded in paraffin, and sectioned according to standard

procedures. Cell nuclei and DNA strand breaks (TUNEL assay) were labeled in some sections with the In Situ Cell Death Detection Kit (Roche Applied Science, Indianapolis, IN), according to manufacturer's instructions. TUNEL-positive cells (brown nuclei) were quantified by averaging the number of brown nuclei in six high-power fields (×400 magnification) per mouse (n = 3 per group), excluding the necrotic area.

Statistical Analysis

Numerical results were expressed as means and 95% confidence intervals (CIs). Statistic significance was evaluated using two-tailed Student *t* tests or analyses of variance. *P* values less than .05 were considered statistically significant.

Results

MET Transcription and Overexpression in Response to IR

We have previously shown that the *MET* proto-oncogene is transcriptionally regulated by specific extracellular and intracellular signals, including growth factors such as its ligand HGF (25) and the oxygen sensor, HIF-1 (26). Here, we investigated modulation of MET expression by exposure to therapeutic doses of IR (up to 10 Gy). In 10 cell lines derived from human breast, lung, prostate, and colon carcinomas, glioma, and neuroblastoma, MET protein levels were substantially increased 24 hours after irradiation (data not shown). In representative cell lines (MDA-MB-231 and MDA-MB-435S human breast cancer cells, and U251 human glioma cells), detailed time-course experiments revealed a biphasic profile of MET protein accumulation. This was characterized by an early peak of approximately fivefold MET induction at around 1–2 hours after irradiation, followed by a similar late peak or a plateau that appeared at 6 hours and diminished 24 hours after irradiation (Figure 1, A and Supplementary Figure 1, A, available online). Dose–response experiments showed that MET induction started between 1 and 5 Gy, and reached a plateau between 5 and 10 Gy, depending on the cell line (Figure 1, B and Supplementary Figure 1, B, available online). In MDA-MB-231, MDA-MB-435S, and U251 cells, MET mRNA accumulation (as shown by Northern blots) and activation of the full-length *MET* promoter (as shown by luciferase reporter assays) were also stimulated by IR treatments (Figure 1, C and D, Supplementary Figure 1, Cand D, available online, and data not shown). Taken together, these data indicated that IR-induced MET overexpression involves a transcriptional mechanism.

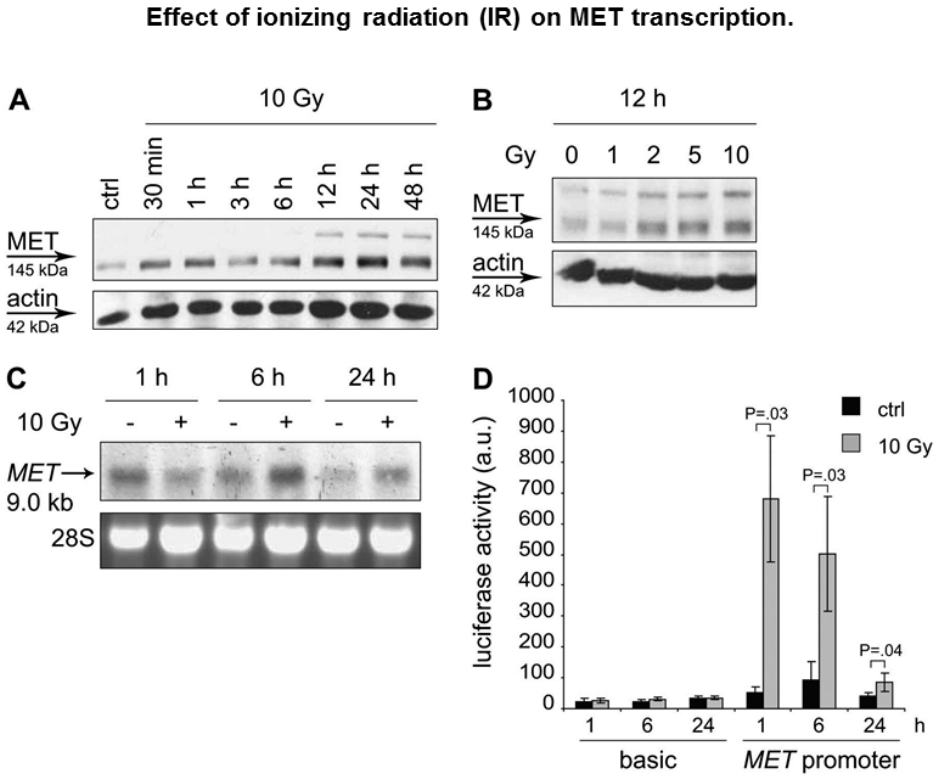

Figure 1

Effect of ionizing radiation (IR) on MET transcription. A) Time course of MET protein expression in MDA-MB-231 cells after irradiation. Cell lysates were analyzed at the indicated time points after irradiation (10 Gy) by immunoblotting. Each blot was cut and the upper parts were incubated with mouse monoclonal anti-MET antibodies. The control lane (ctrl) shows MET expression at time zero. The lower parts of the blots were probed with goat polyclonal anti-actin antibodies as a control for protein loading. Similar results were obtained with MDA-MB-435S and U251 cells (Supplementary Figure 1, A). B) Dose–response of MET protein induction in MDA-MB-231 cells after irradiation. Lysates were analyzed at 12 hours after irradiation (from 0 to 10 Gy) by immunoblotting with anti-MET antibodies. Blots were probed also with anti-actin antibodies as control of protein loading. Similar results were obtained with MDA-MB-435S and U251 cells (Supplementary Figure 1, B). C) Time course of MET mRNA induction in MDA-MB-231 cells after irradiation. RNA was extracted at 1, 6, or 24 hours after irradiation (10 Gy) and examined by Northern blotting using a probe to the entire coding sequence of MET. Ribosomal subunit 28S was measured as control of RNA loading. Similar results were obtained with MDA-MB-435S and U251 cells (Supplementary Figure 1, C,). D) *MET* promoter activity in irradiated MDA-MB-231 cells. Plasmids expressing the luciferase gene under control of the *MET* promoter were transfected and, after 48 hours, cells were irradiated (10 Gy). Then, luciferase activity was measured at 1, 6, or 24 hours and normalized for protein expression. (ctrl = irradiated cells; basic = cells transfected with a plasmid containing a promoterless luciferase gene and treated as above). The means of six samples from two independent experiments and their 95% confidence intervals are shown. (*P*values are derived from two-sided paired *t* tests). Similar results were obtained with MDA-MB-435S cells (Supplementary Figure 1, D,). a.u. = arbitrary units.

MET Signaling in Response to IR

Next, we investigated whether MET signaling was activated by IR. In MDA-MB-231 and U251 cells irradiated with 10 Gy, the overexpressed MET protein, a tyrosine kinase receptor, displayed an increased phosphotyrosine content, as shown by immunoblotting (Figure 2, A and Supplementary Figure 2, A). This was consistent with what we observed in GTL-16 gastric carcinoma cells, in which MET protein overexpression, supported by *MET* gene amplification, was identified as the mechanism responsible for MET kinase constitutive activation and tyrosine phosphorylation (27). Because another possible explanation for MET phosphorylation after irradiation was induction of autocrine HGF signaling, we also analyzed the transcription of HGF in irradiated cells by PCR, and

ruled out the presence of an autocrine loop (Figure 2, E and data not shown). We then investigated activation of signaling downstream of the MET receptor protein by immunoblotting. In irradiated MDA-MB-231 and U251 cells, ligand-independent MET kinase activation resulted in tyrosine phosphorylation of Gab1 (Figure 2, A and Supplementary Figure 2, A). Gab1 is a MET-associated substrate, acting as a multifunctional scaffolding adaptor for the downstream signal transduction pathways, including the Ras/MAP kinase pathway (28). In keeping with increased MET signaling, we showed that MAP kinases were phosphorylated in irradiated MDA-MB-231 and U251 cells, and that their phosphorylation was prevented by the MET-specific tyrosine kinase inhibitor, PHA665752 (29) (Figure 2, B and Supplementary Figure 2, B).

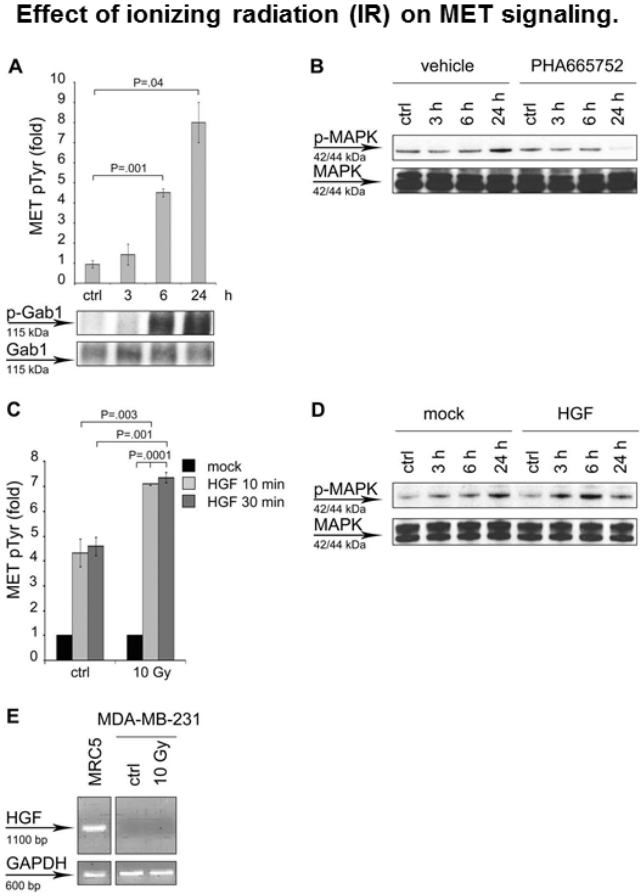

Figure 2

Effect of ionizing radiation (IR) on MET signaling. A) Tyrosine phosphorylation of MET and Gab1 after irradiation. In the upper panel, lysates from MDA-MB-231 cells were immunoprecipitated with anti-MET antibodies at 3, 6, or 24 hours after irradiation (10 Gy) and analyzed by immunoblotting with mouse monoclonal anti-phosphotyrosine (pTyr) antibodies. The same blots were stripped and reprobed with anti-MET antibodies. The amount of MET tyrosine phosphorylation was quantified and normalized against the amount of MET protein detected in immunoblots. The trend of MET phosphorylation, represented as the ratio (MET pTyr fold) of normalized MET phosphorylation in irradiated vs nonirradiated cells, was graphed as the mean of two independent experiments with 95% confidence intervals. MET phosphorylation levels in nonirradiated cells (ctrl) were arbitrarily set to 1. *P* values are from two-sided paired *t* tests. Similar results were obtained with U251 cells (Supplementary Figure 2, A, available online). In the middle panel, on blots of anti-MET immunoprecipitates, anti-phosphotyrosine antibodies recognized a phosphoprotein with a molecular weight corresponding to phosphorylated Gab1 (p-Gab1). In the lower panel, the above blots were stripped and reprobed with rabbit polyclonal antibodies to Gab1, confirming the identity of the protein coprecipitated with MET. B) MET-dependent activation of mitogen-activated protein kinases (MAPK) after irradiation. MDA-MB-231 cells were treated with the MET kinase inhibitor PHA665752 (500 nM) or dimethyl sulfoxide (vehicle), and analyzed 3, 6, or 24 hours after irradiation (10 Gy) by immunoblotting with rabbit polyclonal antibodies recognizing the serine-phosphorylated form of p42/p44 MAP kinases (p-MAPK). The control lane (ctrl) shows MAP kinase phosphorylation at time zero. Blots were stripped and reprobed with rabbit polyclonal anti-MAP kinase antibodies (MAPK) to show equal protein loading. Similar results were obtained with U251 cells (Supplementary Figure 2, B, available online). C) Tyrosine phosphorylation of MET after irradiation and hepatocyte growth factor (HGF) stimulation. Twelve hours after irradiation (10 Gy), MDA-MB-231 cells were treated with HGF (50 ng/mL) for 10 or 30 minutes. Lysates were immunoprecipitated with anti-MET antibodies and analyzed by immunoblotting with

anti-phosphotyrosine antibodies. Blots were stripped and reprobed with anti-MET antibodies. Non-irradiated cells were treated with HGF as above and immunoprecipitated with anti-MET antibodies as a control (ctrl). The amount of MET tyrosine phosphorylation was quantified and normalized against the amount of MET protein detected in immunoblots. The ratio (MET pTyr fold) of normalized MET phosphorylation in HGF-stimulated vs mock-stimulated cells was graphed as the mean of two independent experiments with 95% confidence intervals. MET phosphorylation levels in mock-stimulated cells (mock, black bars) were arbitrarily set to 1. *P* values are derived from two-sided paired *t* tests. Similar results were obtained with U251 cells (Supplementary Figure 2, C, available online). D) Activation of MAP kinases in irradiated and HGF-stimulated cells. MDA-MB-231 cells were stimulated with HGF (50 ng/mL), or mock-stimulated (mock), immediately before irradiation (10 Gy) and analyzed 3, 6, or 24 hours after irradiation by immunoblotting with antibodies recognizing the serine phosphorylated form of p42/p44 MAP kinases (p-MAPK). The control lane (ctrl) shows MAP kinase phosphorylation at time zero. Blots were stripped and reprobed with anti-MAP kinase antibodies (MAPK) to show equal protein loading. Similar results were obtained with U251 cells (Supplementary Figure 2, D, available online). E) HGF mRNA transcription in irradiated MDA-MB-231 cells. HGF mRNA was amplified by endpoint PCR at time zero (ctrl) or 24 hours after irradiation (10 Gy), and resolved in an agarose gel. MRC-5 human fibroblasts were used as the positive control for HGF mRNA transcription.

In irradiated cells, the overexpressed MET tyrosine kinase was not only phosphorylated in the absence of its ligand, but also more sensitive to HGF stimulation. In fact, in MDA-MB-231 or U251 cells, treatment with a nonsaturating dose of HGF (50 ng/mL) increased MET phosphotyrosine content threefold to fourfold in nonirradiated cells, and up to eightfold when such cells were irradiated 12 hours before HGF stimulation (Figure 2, C and Supplementary Figure 2, C). Consistent with these findings, in both irradiated MDA-MB-231 and U251 cells, MET-dependent MAP kinase phosphorylation was further increased if the cells were kept in the presence of HGF (Figure 2, D and Supplementary Figure 2, D).

We also investigated whether IR could increase MET signaling in advance of IR-induced MET protein accumulation. In MDA-MB-231 cells, transient early MET tyrosine phosphorylation was detected, independent of the addition of ligand, within 10 minutes after exposure to IR (Supplementary Figure 2, E). The same phenomenon has been described for the epidermal growth factor receptor (30). The intensity of IR-induced MET phosphorylation was comparable with that elicited by a nonsaturating concentration of HGF (50 ng/mL). In the case of early IR-induced MET phosphorylation, however, combined stimulation by IR and HGF was not synergistic (Supplementary Figure 2, E).

Role of NF-ºB in IR-Induced MET Transcription

Having found that IR induces overexpression of MET at the transcriptional level, we further investigated the mechanisms involved. IR is known to modulate the activity of a few transcription factors including NF-ºB (31). Accordingly, using microarray analysis to determine the transcriptional response to IR, we showed that, in MDA-MB-231 cells, IR induced a prominent early NF-ºB response. For example, nine of the 33 genes with modulated expression at 1 hour after irradiation were NF-ºB targets, which is a frequency approximately 20-fold higher than would be otherwise expected (Supplementary Figure 3 and Supplementary Table 1, available online). Moreover, when nuclear extracts from MDA-MB-231, MDA-MB-435S, or U251 cells were analyzed by immunoblotting in time-course experiments, IR (10 Gy) induced rapid (within 1 hour) and persistent (until 24 hours) nuclear accumulation of the NF-ºB subunit p65/RelA, a hallmark of NF-ºB activation (32) (Figure 3, A and Supplementary Figure 4, A). Finally, in MDA-MB-231 and MDA-MB-435S cells, nuclear p65/RelA was transiently phosphorylated at serine 276 within 1 hour after irradiation (Figure 3, A and Supplementary Figure 4, A, available online). Phosphorylation at this site is known to be induced by ROS via protein kinase A (34), and to promote p65/RelA interaction with the transcriptional coactivator CBP/p300, which is required to support transcription of a subset of early target genes (35). These data indicate that IR promotes functional activation of NF-ºB through nuclear accumulation and early transient phosphorylation of the p65/RelA subunit.

Role of nuclear factor kappa B (NF-κB) in MET transcription induced by ionizing radiation (IR).

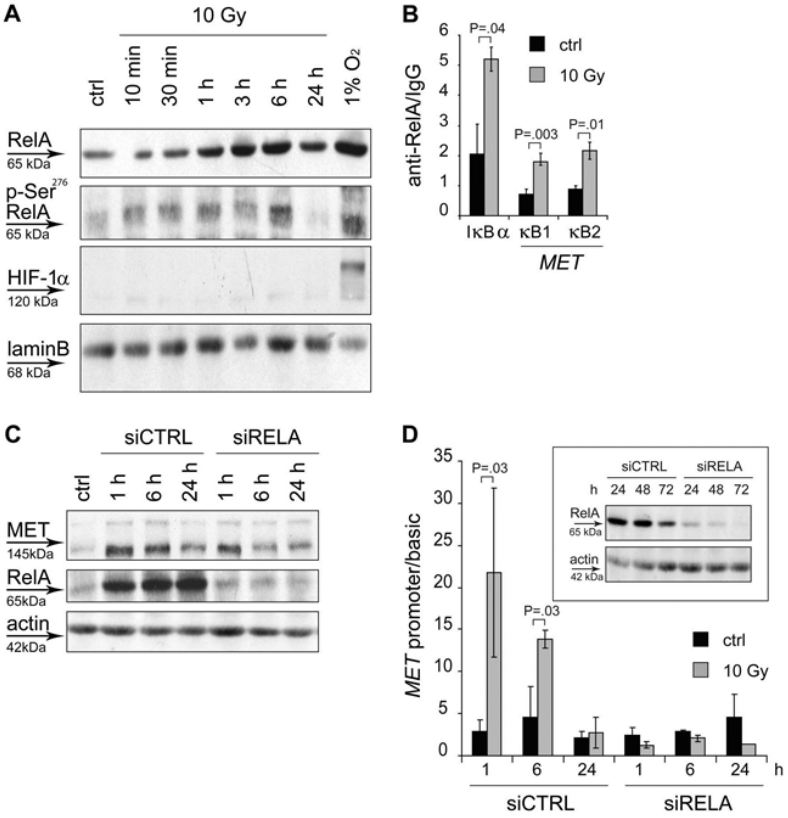

Figure 3

Role of nuclear factor kappa B (NF-ºB) in MET transcription induced by ionizing radiation (IR). A)Accumulation of p65/RelA in cell nuclei after irradiation. Nuclear extracts from MDA-MB-231 cells were immunoblotted with specific antibodies to show the time course of p65/RelA nuclear accumulation (RelA, mouse monoclonal anti-p65/RelA), p65/RelA serine phosphorylation (p-Ser^{276}RelA, rabbit polyclonal anti-phosphoserine 276), and hypoxia inducible factor (HIF)-1± nuclear accumulation (mouse monoclonal anti-HIF-1±), in response to irradiation (10 Gy), or hypoxia (24 hours at 1% O_2). Blots were then stripped and reprobed with mouse monoclonal anti-lamin B as a control of protein loading. Nonirradiated cells at time zero served as a control (ctrl). Similar results were also obtained in MDA-MB-435S and U251 cells (Supplementary Figure 4, A, available online). B) Chromatin immunoprecipitation (ChIP) of NF-ºB response elements in the*MET* promoter. Chromatin was prepared from irradiated MDA-MB-231 cells 3 hours after irradiation (10 Gy) and immunoprecipitated with anti-p65/RelA or nonspecific IgG antibodies. In immunoprecipitates, enrichment of sequences containing each of the two NF-ºB binding sites (ºB1 or ºB2) of the *MET* promoter was evaluated by quantitative polymerase chain reaction amplification. The *NFKBIA* (IºB±) promoter, which contains recognized ºB binding elements (33), was used as positive control for anti-RelA immunoprecipitation. Nonirradiated cells also served as control (ctrl). Ratios between sequence amplification obtained in immunoprecipitates with anti-RelA vs immunoprecipitates with nonspecific IgG are shown (means of three replicates of one experiment with 95% confidence intervals, two-sided paired *t* tests). C) RelA-dependent expression of MET after irradiation. MDA-MB-231 cells were transfected with silencing RNA (siRNA) against p65/RelA (siRELA) or control siRNA (siCTRL) and irradiated (10 Gy). Lysates were analyzed 1, 6, or 24 hours after treatment by immunoblotting with anti-MET (MET) or anti-p65/RelA (RelA) antibodies. The control lane (ctrl) shows MET or p65/RelA expression in mock-transfected cells at time zero after irradiation. Blots were also probed with anti-actin as control of protein loading. Similar results were obtained with MDA-MB-435S and U251 cells (Supplementary Figure 4, B, available online). D) Luciferase activity driven by the *MET* promoter in irradiated cells lacking p65/RelA. MDA-MB-231 cells were transfected with a plasmid expressing the luciferase gene under control of the *MET* promoter and with siRNA against p65/RelA (siRELA) or control siRNA (siCTRL). After 48 hours, cells were irradiated (10 Gy; ctrl = nonirradiated cells). Luciferase activity was measured 1, 6, or 24 hours after irradiation, and normalized for protein expression. In parallel, cells transfected with a plasmid containing a promoterless luciferase gene (basic) and the above siRNA were irradiated, and luciferase was measured as above. Ratios of luciferase activity in cells containing the *MET*promoter vs the basic plasmid are shown (means of nine samples from three independent experiments, with 95% confidence intervals, *P* values from two-sided paired *t* tests). The inset panel presents immunoblots showing p65/RelA protein after siRNA transfection, and actin as control of protein loading.

To determine whether NF-ºB could bind the MET promoter, we performed ChIP experiments. Through in silico analysis, we had identified two putative NF-ºB binding sites in the

human *MET* gene promoter: ºB1, located at −1349 to −1340 bp, and ºB2, located at −1150 to −1137 bp with respect to the transcription start site (23). Interestingly, the ºB2 site is highly conserved and functional in the murine *met* promoter (Supplementary Figure 5, available online) (36). ChIP experiments in MDA-MB-231 cells showed that association of p65/RelA to either site was more than doubled in cells exposed to irradiation (10 Gy) (Figure 3, B), indicating that MET expression is transcriptionally controlled by NF-ºB in irradiated cells. These findings prompted us to investigate whether NF-ºB is absolutely required for MET induction by IR. p65/RelA is involved in the formation of most NF-ºB heterodimers and is thus critical for NF-ºB-driven transcriptional activity (35,37). We therefore inhibited p65/RelA expression in MDA-MB-231, MDA-MB-435S, or U251 cells through siRNA transfection. Cells were then irradiated (10 Gy) and lysates were analyzed by immunoblotting from 10 minutes to 24 hours after irradiation. These experiments showed that, in the absence of p65/RelA, IR could not induce MET protein expression (Figure 3, C and Supplementary Figure 4, B, available online). To investigate whether lack of MET induction occurred at transcriptional level, luciferase reporter assays with the full-length *MET*promoter were performed in MDA-MB-231 cells transfected with siRNA against p65/RelA. These assays showed that, in the absence of p65/RelA, IR could not induce the activity of the *MET* promoter (Figure 3, D). Taken together, these data provide convincing evidence that IR-induced MET overexpression requires activation of the transcription factor NF-ºB.

We also considered the involvement of HIF-1 in IR-induced MET transcription because HIF-1 is a prominent regulator of MET expression (26), and it was shown to be activated in irradiated cells as a result of ROS formation (38). However, the contribution of HIF-1 was minimal, as shown by complementary approaches. First, MDA-MB-231 and MDA-MB-435S cells were irradiated (10 Gy), and nuclear extracts were analyzed by immunoblotting from 10 minutes to 24 hours after irradiation. IR did not induce nuclear accumulation of the HIF-1± subunit, which is the hallmark of HIF-1 activation, as observed in control cells cultured at a low oxygen concentration (1%) (Figure 3, A and Supplementary Figure 4, A, available online). The lack of HIF-1 activation was not due to weak ROS production in irradiated cells because ROS were increased, on average, by 25% (95% CI = 19% to 31%) at 15 minutes after exposure to 10 Gy. By comparison with previous observations in cell lines exposed to 1–10 Gy, this increase was estimated to correspond to an average of 80% ROS induction within 2–5 minutes after irradiation (39). Moreover, in luciferase reporter assays, IR could not activate the so-called “minimal” *MET* promoter (a sequence including nucleotides from −295 to +353 with respect to the transcription start site) (23). This sequence includes the two functional hypoxia responsive elements and the AP-1 site that we previously showed as responsible for hypoxia-induced *MET* transcription (26) (data not shown). Taken together, these data indicate that HIF-1 is not implied in induction of MET transcription by IR. However, we observed that hypoxia induced nuclear translocation and serine phosphorylation of p65/RelA (Figure 3, Aand Supplementary Figure 4, A, available online), consistent with recent findings (40).

Finally, we also ruled out that transcription factor p53, another prominent IR target (11), was involved in IR-induced MET transcription. In fact, MDA-MB-435S, MDA-MB-231, and U251, the three cell lines that displayed the highest MET induction by IR, harbor p53-inactivating mutations (G266E, R280K, and R273H, respectively) (41,42). Moreover, unlike the murine promoter (43), the human *MET* promoter was not induced by constitutively active forms of p53, as observed by us and others (Selma Pennacchietti, Paolo Michieli, and Paolo M. Comoglio, IRCC-Institute for Cancer Research at Candiolo, University of Turin Medical School, Candiolo, Italy; Jinhyang Choi, and Alexander Y. Nikitin, Department of Biomedical Sciences, Cornell University, Ithaca, NY, personal communications).

Role of ATM Kinase and TNF-± Signaling in IR-Induced NF-ºB Activation

NF-ºB is a target of several pathways that can be initiated by both extracellular and intracellular signals (32). Mechanisms of intracellular activation include those elicited by protein kinase ATM following detection of DNA damage (11,44). To investigate whether MET induction by IR relies on activation of the ATM kinase, MDA-MB-231, MDA-MB-435S, or U251 cells were treated with the ATM inhibitor, CGK733 (10 µM) (45), 4 hours before irradiation. Extracts were analyzed from 30 minutes to 6 hours after irradiation (10 Gy) by immunoblotting, to detect threonine phosphorylation of the specific ATM substrate Chk2, nuclear translocation of p65/RelA, and expression of MET. CGK733 prevented Chk2 phosporylation, indicating ATM inhibition, and abolished p65/RelA nuclear translocation and MET protein overexpression. These data suggest that ATM kinase signaling is required for IR-induced MET overexpression (Figure 4, A, Supplementary Figure 6, A, available online, and data not shown).

Role of ataxia telangiectasia mutated (ATM) kinase signaling and tumor necrosis factor alpha (TNF-α) autocrine loop in ionizing radiation (IR)-induced nuclear factor kappa B (NF-κB) activation.

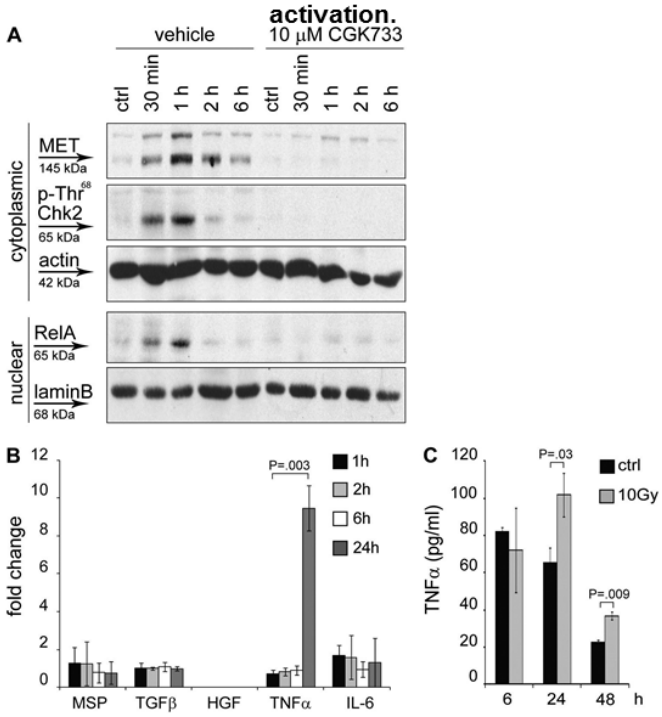

Figure 4

Role of ataxia telangiectasia mutated (ATM) kinase signaling and tumor necrosis factor alpha (TNF-±) autocrine loop in ionizing radiation (IR)-induced nuclear factor kappa B (NF-ºB) activation. A) Effect of the ATM kinase inhibitor, CGK733, on MET, Chk2, and p65/RelA in irradiated cells. MDA-MB-231 cells were treated with CGK733 (10 µM) or dimethyl sulfoxide (vehicle) for 4 hours and then irradiated (10 Gy). Cytoplasmic or nuclear extracts obtained from 30 minutes to 6 hours after irradiation were analyzed by immunoblotting with specific antibodies to show MET expression, Chk2 threonine phosphorylation (p-Thr^{68} Chk2, rabbit polyclonal anti-phospho Chk2 antibodies), and p65/RelA (RelA) nuclear accumulation. Blots were stripped and reprobed with anti-actin or anti-lamin B antibodies as controls of protein loading. Nonirradiated cells at time zero served as control (ctrl). Similar results were obtained with MDA-MB-435S and U251 cells (Supplementary Figure 6, A, available online, and data not shown). B) Transcription of growth factors and cytokines in irradiated MDA-MB-231 cells. RNA levels were measured by quantitative polymerase chain reaction at the indicated time points after irradiation (10 Gy). The graph shows the fold change in RNA content in irradiated vs nonirradiated cells (means of nine samples from three independent experiments with 95% confidence intervals; *P* values from two-sided paired *t* tests). Similar results were obtained with MDA-MB-435S and U251 cells (Supplementary Figure 6, B, available online, and data not shown). C) TNF-±

secretion by irradiated MDA-MB-231 cells. Cell culture media were removed 6, 24, or 48 hours after irradiation (10 Gy), and TNF-± concentration (pg/mL) was measured by enzyme-linked immunosorbent assays. Nonirradiated cells served as control (ctrl). The graph shows a mean of six samples from two independent experiments, with 95% confidence intervals. *P* values were derived from two-sided paired *t* tests. Similar results were obtained with MDA-MB-435S cells (Supplementary Figure 6, C, available online). MSP = macrophage stimulating protein; TGF-² = transforming growth factor ²; IL-6 = interleukin 6.

It is also known that NF-ºB induces the expression of cytokines, including TNF-± (33), that promote a positive-feedback loop to increase NF-ºB activity. Therefore, we investigated expression of cytokines by irradiated MDA-MB-231, MDA-MB-435S, or U251 cells in time-course experiments. As shown by quantitative PCR, TNF-± transcription was increased in all three cell lines, peaking at different time points (from 2 to 24 hours) after irradiation (10 Gy) (Figure 4, B, Supplementary Figure 6, B, available online, and data not shown). In MDA-MB-231 and MDA-MB-435S cells, we also measured TNF-± release into the culture medium by ELISA and found increased secretion of the protein at 24–48 hours after irradiation (10 Gy) (Figure 4, C and Supplementary Figure 6, C, available online). These data suggest that, in irradiated cells, MET expression can be supported by a TNF-± autocrine loop. By contrast, transcription of other NF-ºB targets, such as HGF, interleukin 6, or other proinvasive cytokines such as MSP and TGF-², was not induced by irradiation (Figure 4, B, Supplementary Figure 6, B, available online, and data not shown). The lack of HGF induction may be explained by the fact that the HGF gene is likely to undergo epigenetic silencing during cell fate determination in cells of epithelial or neural origin. Conversely, the *MET* gene appears to be epigenetically silenced in cells of mesenchymal origin, which expresses HGF, but not MET (see "Discussion"). Consistent with this pattern, in the normal fibroblast cell line MRC-5, irradiation (10 Gy) increased HGF transcription up to threefold (Supplementary Figure 6, D, available online), but did not affect MET transcription (data not shown). Taken together, these results suggest that irradiation of both tumor and stromal cells induce the expression of cytokines that increase MET expression and activation (see "Discussion").

Role of MET in IR-Induced Invasive Growth

IR-induced MET overexpression resulted in substantially increased ligand-independent MET kinase activation (Figure 2, A and Supplementary Figure 2, A, available online). We therefore investigated whether IR-induced MET overexpression and activation were followed by MET-associated biological responses, which include invasive growth.

We first performed wound healing assays, as an in vitro model to assess the propensity of irradiated cells overexpressing MET for invasive growth. Subconfluent monolayers of MDA-MB-231, MDA-MB-435S, or U251 cells were scratched to produce a wound, and then irradiated (10 Gy). Irradiated cells, compared with nonirradiated cells, more readily performed the healing program, by detaching from the edge of the wound, and migrating throughout the scratched area (Figure 5, A and data not shown). This response, monitored for 24 hours, was similar to that stimulated by HGF, aka "Scatter Factor" because it promotes cell dissociation and motility (46) (data not shown). The healing response elicited by IR was not due to induction of an HGF autocrine loop, as assessed by quantitative PCR (Figure 4, B; Supplementary Figure 6, B, available online, and data not shown). Reconstitution of the wounded monolayer by irradiated cells was, however, fully prevented by adding the MET inhibitor, PHA665752, to cell monolayers immediately before irradiation (Figure 5, A and data not shown), indicating that MET signaling was an absolute requirement for IR-induced invasive growth.

Role of MET in ionizing radiation (IR)-induced invasive growth.

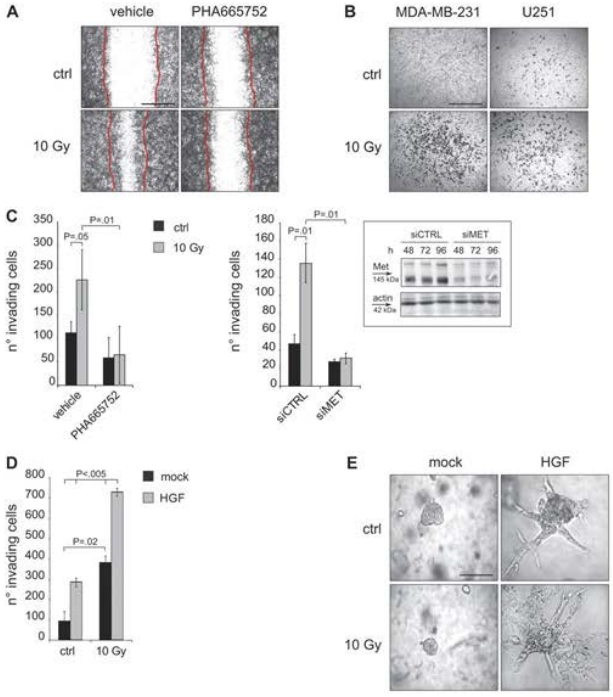

Figure 5

Role of MET in ionizing radiation (IR)-induced invasive growth. A) Effect of MET inhibition on IR-induced cell migration in the wound healing assay. MDA-MB-231 monolayers were scratched, irradiated (10 Gy; ctrl = nonirradiated cells), kept in the presence of the MET inhibitor, PHA665752 (500 nM), or dimethyl sulfoxide (DMSO) (vehicle) for 24 hours, and micrographs were taken at ×100 magnification. Lines indicate wound margins at time zero. Scale bar: 100 µm. Similar results were obtained in MDA-MB-435S and U251 cells (data not shown). B) IR-induced invasion in the transwell assay. MDA-MB-231 or U251 cells were seeded onto Matrigel-coated transwell filters, and irradiated (10 Gy; ctrl = nonirradiated cells). After 24 hours, cells that invaded the filters were stained with crystal violet and micrographs were taken at ×100 magnification. Scale bar: 100 µm. C) Effect of MET inhibition on IR-induced cell invasion in the transwell assay. Assays were performed as in (B) with cells undergoing MET inhibition as follows. In the left panel, cells were supplied with PHA665752 (500 nM) or DMSO (vehicle) immediately before irradiation, and kept in the presence of the inhibitor during the transwell assay. In the right panel, cells underwent irradiation and transwell assay 48 hours after transfection of silencing RNA (siRNA) against MET (siMET) or control siRNA (siCTRL). Both graphs represent the number of MDA-MB-231 cells that invaded Matrigel-coated transwell filters 24 hours after irradiation (10 Gy; ctrl = nonirradiated cells). The means of six samples from three independent experiments, with 95% confidence intervals, are shown. *P* values are from two-sided paired *t* tests. In the inset, an immunoblot shows MET expression at the indicated time points after transfection of siMET or siCTRL. Blots were probed also with anti-actin as control of protein loading. Similar results with PHA665752 were obtained in U251 cells (Supplementary Figure 7, A, available online). D) Hepatocyte growth factor (HGF) stimulated invasiveness in the transwell assay. Experiments were performed as in (B) except in that MDA-MB-231 cells received HGF (50 ng/mL) in place of the MET inhibitor, or were mock treated during the transwell assay. The graph represents the number of MDA-MB-231 cells that invaded Matrigel-coated transwell filters 24 hours after irradiation (10 Gy; ctrl = nonirradiated cells). The means of six samples from two independent experiments, with 95% confidence intervals, are shown. *P* values are from two-sided paired *t* tests. Similar results were obtained with U251 cells (Supplementary Figure 7, B, available online). E) Effect of IR on MET-mediated branching morphogenesis. MDA-MB-435S cells were embedded in a three-dimensional collagen matrix to form multicellular spheroids. Cells were then irradiated (10 Gy; ctrl = nonirradiated cells) and cultured in the presence of HGF (50 ng/mL, purified as a recombinant protein from baculovirus-infected SF9 insect cells) or mock medium (conditioned medium from noninfected SF9 insect cells) for 7 days. As a control of normal branching morphogenesis, nonirradiated cells were cultured in the presence of HGF. Micrographs were taken at ×200 magnification 7 days after irradiation. Scale bar: 50 µm.

MDA-MB-231, MDA-MB-435S, or U251 cells were then studied in invasion assays (47) to measure their ability to traverse an artificial basement membrane in vitro in response to irradiation (10 Gy). Cells were seeded in transwell chambers, onto filters coated with Matrigel. Irradiated cells

displayed substantially increased ability to invade the filters compared with nonirradiated cells (Figure 5, B and data not shown), again mimicking the behavior evoked by HGF in nonirradiated cells (48). Like IR-stimulated wound healing, the IR-stimulated proinvasive effect was dependent on MET because it could be abolished either by addition of the MET-specific inhibitor, PHA665752 (Figure 5, C and Supplementary Figure 7, A, available online) or by addition of siRNA against MET (Figure 5, C and data not shown). Having shown that IR and HGF synergized to induce MET signaling (Figure 2, C and D and Supplementary Figure 2, C and D, available online), we investigated whether they could synergize to induce cell invasion as well. We therefore irradiated (10 Gy) MDA-MB-231 or U251 cells seeded on Matrigel-coated transwell filters, and we kept them in the presence of HGF (50 ng/mL) for 24 hours. Cells that received both IR and HGF displayed increased ability to invade the filters, compared with cells that received IR or HGF alone (Figure 5, D and Supplementary Figure 7, B, available online).

Effect of IR on MET-Mediated Morphogenesis

HGF stimulates branching morphogenesis, a complex physiological process that includes cell migration, proliferation, and spatial reorganization, to generate hollow branched tubules during development (49). Some cell lines, like MDA-MB-435S cells, can fully execute the branching morphogenesis program in vitro.

We investigated whether IR could induce or interfere with the branching morphogenesis process. We therefore embedded MDA-MB-435S cells into a three-dimensional collagen matrix, to form multicellular spheroids. Exposure to IR alone (10 Gy) did not induce branching morphogenesis, which is not surprising, as the transient MET overexpression and activation induced by IR is likely insufficient to support the entire process, which requires MET activation sustained over several days. Moreover, while nonirradiated cells kept in the presence of HGF for 7 days formed normal branching tubules, irradiated cells in the same conditions built tubules that displayed remarkable structural alterations, as cells seemed to disengage from the external surface and disseminate into the surrounding matrix (Figure 5, E). This phenotype was reminiscent of the “tridimensional scatter” that has been described as a form of aberrant, pro-invasive morphogenesis that occurs in response to TNF-± (50).

Contribution of MET Inhibition to IR-Induced Apoptosis and Proliferative Arrest

As part of the invasive growth program, MET emanates powerful antiapoptotic signals through sustained activation of downstream signaling pathways [reviewed in (51)]. Therefore, we reasoned that increased MET expression could prevent cell death induced by irradiation, and conversely, that MET inhibition could increase the efficacy of radiotherapy. To explore this hypothesis, we assessed the viability of irradiated MDA-MB-231, MDA-MB-435S, or U251 cells by evaluating cell metabolic activity. Culture in the presence of the MET inhibitor PHA665752, and conditions nonpermissive for proliferation, reduced cell viability by more than 50% at 48 hours after irradiation (10 Gy) (Figure 6, Aand Supplementary Figure 7 C, available online). Radiation sensitivity of the above cell lines was independent of the degree of confluence (data not shown). To examine whether the reduced viability of irradiated cells treated with the MET inhibitor was due to increased apoptosis, we measured the levels of active caspase-3 by immunoblotting. At 6 hours after irradiation (10 Gy), MDA-MB-231, MDA-MB-435S, or U251 cells treated with PHA665752 displayed a more than doubled content of active caspase-3 as compared with irradiated cells treated with the vehicle (Figure 6, B and data not shown). Also, treatment with PHA665752 alone induced a slight accumulation of active caspase-3 (Figure 6, B); however, it did not substantially affect cell viability (Figure 6, A and Supplementary Figure 7, C, available online). We thus concluded that decreased viability of irradiated cells treated with the MET inhibitor was likely due to increased apoptosis.

Contribution of MET inhibition to ionizing radiation (IR)-induced apoptosis and proliferative arrest.

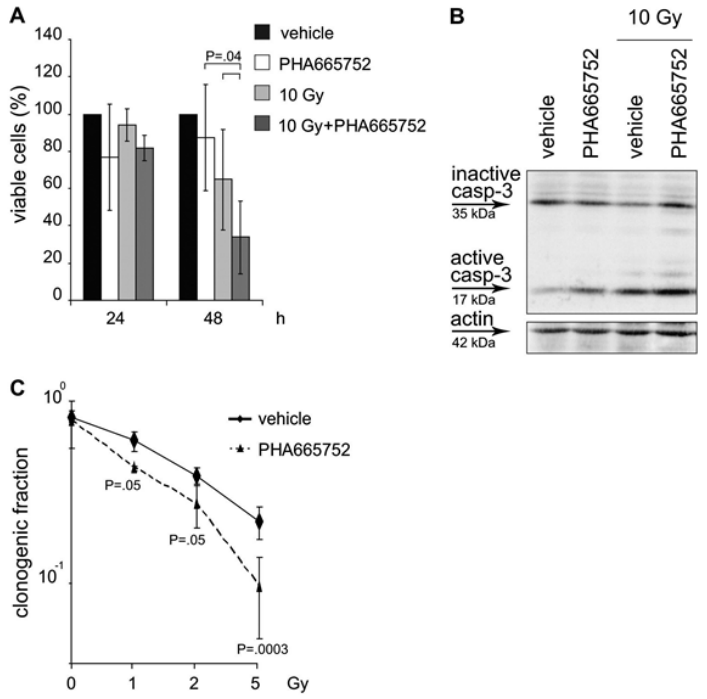

Figure 6

Contribution of MET inhibition to ionizing radiation (IR)-induced apoptosis and proliferative arrest. A) MET inhibition and viability of irradiated cells. MDA-MB-231 cells were grown to confluence, serum starved, and irradiated (10 Gy). Cells were kept in the presence of either the MET inhibitor PHA665752 or DMSO (vehicle), which were added immediately before irradiation, for up to 48 hours. Cell viability was evaluated by measuring ATP production 24 or 48 hours after irradiation. The graph shows means of nine samples from three independent experiments with 95% confidence intervals. *P* values are from two-sided paired *t* tests. Survival of nonirradiated cells kept in the presence of the vehicle was arbitrarily set to 100%. Similar results were obtained with MDA-MB-435S and U251 cells (Supplementary Figure 7, C, available online). B) Met inhibition and caspase-3 activation in irradiated cells. MDA-MB-231 cells were irradiated (10 Gy) and kept in the presence of PHA665752 (500 nM) or dimethyl sulfoxide (DMSO) (vehicle). As a control, nonirradiated cells received the same treatments. After 6 hours, lysates were analyzed by immunoblotting with rabbit polyclonal anti-caspase 3 antibodies recognizing either the active (active casp-3) or the inactive caspase-3 (inactive casp-3) forms. Blots were stripped and reprobed with anti-actin antibodies as a control of protein loading. Similar results were obtained with MDA-MB-435S and U251 cells (data not shown). C) MET inhibition and clonogenicity of irradiated cells. MDA-MB-231 cells were seeded at low density, irradiated (1–5 Gy) and cultured in the presence of PHA665752 (500 nM, dotted line) or DMSO (vehicle, solid line) for 15 days. The clonogenic fraction (percentage of colonies containing more than 50 cells) was calculated as described in "Methods". The graph shows means of eight samples from two independent experiments with 95% confidence intervals. *P* values were from two-way analysis of variance. Similar results were obtained with U251 cells (data not shown).

Moreover, we investigated whether MET inhibition impaired the proliferative ability of cells surviving irradiation. Therefore, we performed a clonogenic assay, by plating MDA-MB-231 or U251 cells at low density. Cells were exposed to increasing doses of IR (1–5 Gy), and cultured in the presence of PHA665752 or vehicle. After 15 days, the clonogenic fraction [ie, the percentage of colonies containing more than 50 cells, calculated as described in detail in "Methods" and (24)] was substantially reduced in cells that received both IR and PHA665752, as compared with cells that received IR or PHA665752 alone. Notably, the MET inhibitor halved the IR dose required to obtain a similar reduction in the number of colonies (Figure 6, C and data not shown). Taken together, these results indicated that inhibition of MET was able to sensitize cells to ionizing radiation, likely

by decreasing their resistance to IR-induced apoptosis, and, as shown by clonogenic experiments, by reducing their ability to resume proliferation after treatment.

Contribution of MET Inhibition to Radiosensitization of Tumor Xenografts

To determine whether MET inhibition can radiosensitize tumor cells in vivo, we transplanted U251 human glioma cells and MDA-MB-231 human breast cancer cells into subcutaneous sites on the right flanks of immunocompromised mice. Established tumors were then treated with different irradiation protocols. Mice with U251 tumors received a single dose of 5 Gy at day 0, whereas mice with MDA-MB-231 tumors received a fractionated dose of 4.5 Gy (1.5 Gy per fraction, each administered on days 0, 2, and 4). Mice were then treated by daily administration of the novel MET inhibitor, JNJ-38877605 (50 mg/kg), until the end of the experiments. JNJ-38877605 displays selectivity and inhibitory activity against MET that is comparable to or higher than PHA665752 [Supplementary Figure 8, available online and (15,52,53)]. JNJ-38877605 was chosen because, unlike PHA665752, it can be administered orally, and because PHA665752 caused tissue damage at the site of injection in a substantial percentage of mice (approximately 50%, our unpublished observation). While radiotherapy alone caused tumor growth arrest at best, association of radiotherapy with the MET inhibitor induced statistically significant further decrease of U251 tumors (at day 13, relative to mean tumor volume at day 0, volume increase of tumors treated with vehicle = 438%, with JNJ-38877605 = 398%, with IR = 151%, with JNJ-38877605 + IR = 76%; difference, vehicle vs JNJ-38877605 = 40%, 95% CI = −17% to 97%, $P = .65$; difference, JNJ-38877605 vs JNJ-38877605 + IR = 322%, 95% CI = 298% to 346%, $P < .001$; difference, IR vs JNJ-38877605 + IR = 75%, 95% CI = 59% to 91%, $P = .01$) (Figure 7, A). Interestingly, association with the MET inhibitor could also switch an ineffective low-dose irradiation protocol (4.5 Gy fractionated) into a treatment capable of reducing MDA-MB-231 tumor volume by an average 75% (at day 7, relative volume increase of tumors treated with vehicle = 169%, with JNJ-38877605 = 136%, with IR = 131%, with JNJ-38877605 + IR = 34%; difference, vehicle vs JNJ-38877605 = 33%, 95% CI = 8% to 58%, $P = .33$; difference, JNJ-38877605 vs JNJ-38877605 + IR = 102%, 95% CI = 86% to 118%, $P = .005$; difference, IR vs JNJ-38877605 + IR = 97%, 95% CI = 80% to 114%, $P = .006$) (Figure 7, B). We also investigated whether tumor treatment with the MET inhibitor increased IR-induced cell apoptosis. Established xenografts of MDA-MB-231 cells were irradiated with a single dose of 5 Gy, tumors were explanted on days 2, 4, and 6 after irradiation, and tumor sections were stained with TUNEL assay. The number of apoptotic cells was statistically significantly increased in tumors undergoing combined therapy with respect to either treatment with irradiation or MET inhibitor alone (at day 6, number of TUNEL-positive cells per high-power field after treatment with vehicle = 0, with JNJ-38877605 = 3, with IR = 122, with JNJ-38877605 + IR = 243; difference, JNJ-38877605 + IR vs JNJ-38877605 = 240, 95% CI = 233 to 247, $P < .001$; difference, JNJ-38877605 + IR vs IR = 121, 95% CI = 97 to 145, $P = .008$) (Figure 7, C and D).

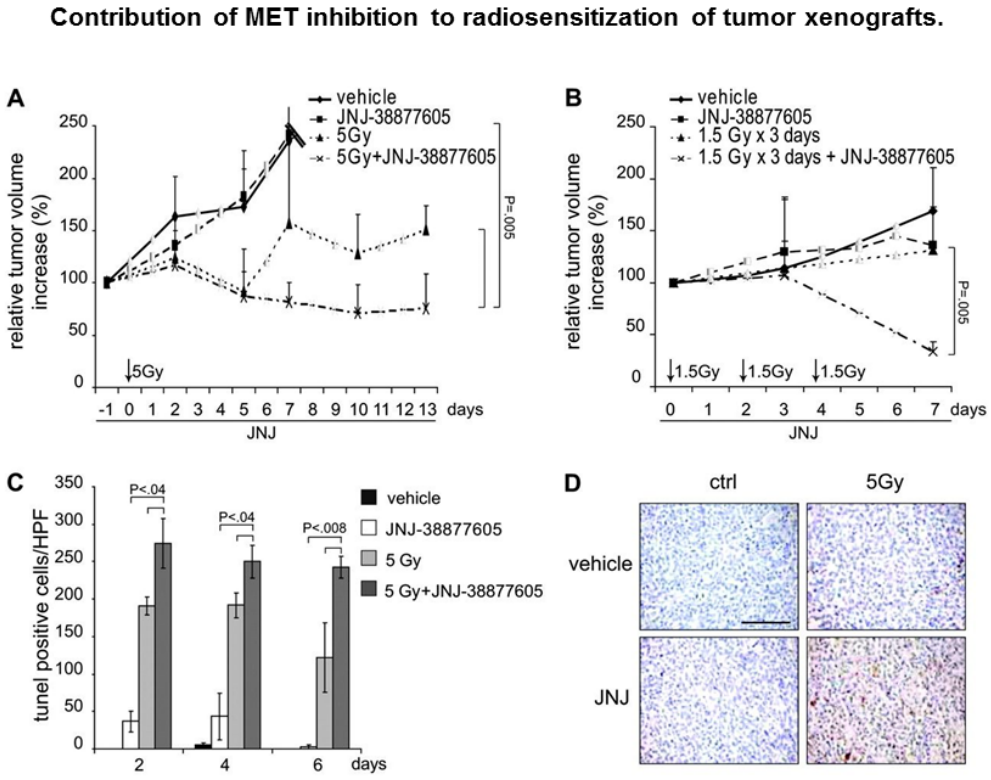

Figure 7

Contribution of MET inhibition to radiosensitization of tumor xenografts. A) Radiosensitization of U251 xenografts. U251 cells were injected subcutaneously into immunocompromised CD1-nu$^{-/-}$ mice. Established tumors received a single dose of 5 Gy at day 0, and mice were treated by daily oral administration of the MET inhibitor, JNJ-38877605 (50 mg/kg), or vehicle, from day −1 to day 13. Nonirradiated mice were treated as above. Tumor diameters were measured every 3 days with a caliper. The graph represents the relative tumor volume increase as means with 95% confidence intervals (n = 6 mice per group; *P* values from two-sided paired *t* tests). Shaded symbols= extrapolated values. B) Radiosensitization of MDA-MB-231 xenografts. MDA-MB-231 cells were injected subcutaneously into immunocompromised NOD/SCID mice. Established tumors received a fractionated dose of 4.5 Gy (1.5 Gy per fraction, each administered on days 0, 2, and 4), and mice were treated by daily oral administration of the MET inhibitor, JNJ-38877605 (50 mg/kg), or vehicle, from days 0 to 7. Nonirradiated mice were treated as above. Tumor diameters were measured every 3 days with a caliper. The graph represents the relative tumor volume increase as means with 95% confidence intervals (n = 5 mice per group, two-sided paired *t* tests). Shaded symbols = extrapolated values. C) Apoptosis in MDA-MB-231 xenografts. Mice with established MDA-MB-231 tumors were irradiated with a single IR dose (5 Gy) and daily treated with JNJ-38877605 (50 mg/kg) or vehicle. Nonirradiated mice were treated as above (n = 9 mice per group). Tumors were explanted on day 2, 4, or 6 after irradiation, sections were stained with a TUNEL assay to detect apoptotic cells, and the number of TUNEL-positive (apoptotic) cells per high-power field (HPF) (×400 magnification) was counted. The graph shows means of six HPF per mouse (n = 3) with 95% confidence intervals (*P* values from two-sided paired *t*tests). D) Representative images of MDA-MB-231 tumors treated and stained with TUNEL assay as in (C), and photographed at ×200 magnification 6 days after treatment. Brown nuclei indicate apoptotic cells. Scale bar: 50 μm. ctrl = nonirradiated cells.

Discussion

In addition to damaging intracellular targets, IR (mostly through generation of ROS) tunes the activity of regulatory molecules, which control the stress-and-recovery biological response. Increased transcription of the *MET* oncogene and activation of its signaling activity emerged as crucial events in this response, resulting in the execution of a prosurvival and regenerative program that counteracts radiation-induced damage.

In this article, we have shown that IR-induced transcription of *MET* was controlled by a signal transduction pathway elicited by the protein kinase ATM following the detection of DNA damage.

This pathway includes nuclear export of the ATM kinase and release of the transcription factor NF-ºB from inhibition (44). Activation of NF-ºB by DNA damage is known to play a key role in the defensive response against radiation because NF-ºB is a prominent regulator of antiapoptotic genes (54,55), and cell survival promoted by NF-ºB has been proposed to be effective enough to induce “adaptive resistance” of cancer cells to radiotherapy (56). Here, we have shown that the adaptive response to radiation sustained by NF-ºB was mediated by the *MET* proto-oncogene.

MET induction by IR was a biphasic transcriptional event, mediated by binding of NF-ºB to the two NF-ºB–specific response elements located in the *MET* promoter. The early transcriptional response that occurred within 1–2 hours after irradiation likely relied on NF-ºB activation by intracellular signaling driven by the DNA damage sensor, ATM. At later times, increased MET transcription was sustained (more than 24 hours) and was likely to be supported by multiple extracellular (paracrine) signals that also activate NF-ºB [reviewed in (57)]. By analyzing a panel of candidate cytokines, we found that irradiated cancer cells expressed and secreted TNF-±, which, on the one hand, is a NF-ºB target, and, on the other hand, stimulates NF-ºB transcriptional activity (33). We suggest that, in living tissues, irradiation induces autocrine or paracrine signaling by TNF-± that sustains NF-ºB activation and induces waves of survival signals throughout the damaged tissue.

Among the outcomes of IR-induced NF-ºB activation, MET overexpression resulted in ligand-independent activation of MET signaling, and activation of critical downstream effectors, including Gab1, a MET-specific multifunctional signaling adaptor protein, and the Ras-MAP kinase pathway. In addition, the overexpressed MET receptor was hypersensitive to HGF stimulation, and therefore, in irradiated cells, MET signaling and biological responses to HGF were hyperactivated. Interestingly, like *MET*, the *HGF* gene is an NF-ºB target (33). However, unlike *MET*, the *HGF* gene was not induced by irradiation in cancer cells of epithelial or neuroectodermal origin. On the contrary, HGF was induced by irradiation in stromal cells, which normally secrete it for paracrine stimulation of epithelial cells (58). We conclude that, in human cancers, IR can support MET activation through multiple mechanisms (Figure 8), which include the following: 1) *MET* transcriptional upregulation initiated by cell-autonomous events (ATM activation) and supported by autocrine–paracrine mechanisms (TNF-±), 2) ligand-independent activation of MET, caused by overexpression, and 3) ligand-dependent hyperactivation of MET, mediated by HGF released from stromal cells.

Effects of ionizing radiation (IR) on transcription and activation of the MET signaling pathway.

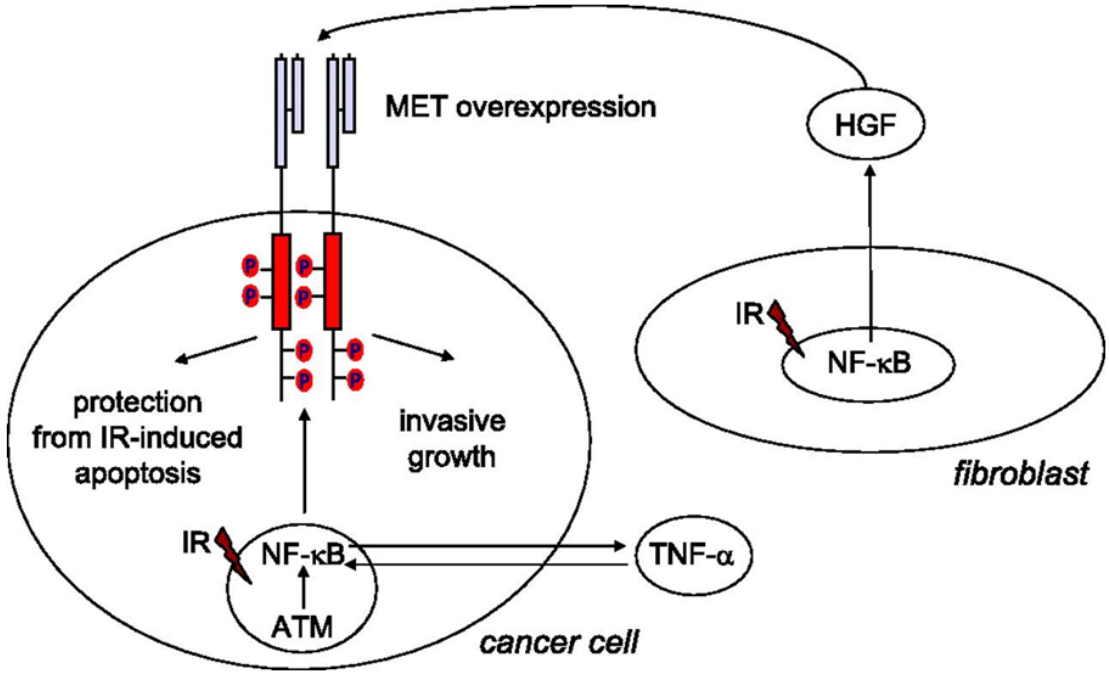

Figure 8

Effects of ionizing radiation (IR) on transcription and activation of the MET signaling pathway. IR activates a signaling cascade initiated by the DNA-damage sensor ataxia telangiectasia mutated (ATM), ending in activation of the transcription factor nuclear factor kappa B (NF-ºB), which leads to overexpression of MET at the cell surface. Signaling via NF-ºB is amplified by a positive-feedback loop mediated by tumor necrosis factor ± (TNF-±). The overexpressed MET tyrosine kinase is activated in the absence of its ligand hepatocyte growth factor (HGF) and is also sensitized to HGF, which is secreted by irradiated stromal cells (fibroblasts), likely as result of NF-ºB activation. MET transduces signals that promote invasive growth and protection from IR-induced apoptosis, thus supporting cancer cell radioresistance and dissemination.

In irradiated tissues, increased expression of the NF-ºB target genes *MET*and *HGF* promotes the execution of a complex program, controlling cell survival and invasion, which acts as a double-edge sword: in normal tissues, this program promotes recovery from damage, in cancer cells, progression toward malignancy. As we showed, on the one hand, IR-induced MET overexpression and activity enabled cells to heal wounded monolayers. On the other hand, it stimulated cells to invade artificial basement membranes, an activity predictive of invasive/metastatic ability in vivo (47). Even more strikingly, in irradiated cells, the physiological process of HGF-induced branching morphogenesis was turned into disorganized cell dissemination throughout a tridimensional matrix. In all cases, although several NF-ºB target genes were expressed in irradiated cells, we showed, through inhibition of MET expression or activity, that MET was required for both physiological invasive growth (wound healing) and malignant invasive growth (invasiveness). We thus speculate that the reported aggressiveness of tumors relapsing after irradiation likely involves activation of the invasive growth program under a tight control of the *MET* oncogene.

We also showed that MET kinase inhibition in association with radiotherapy induced tumor growth arrest and regression in vivo, likely as a result of impaired cell survival and clonogenic ability, as measured in vitro and in vivo. This has important therapeutic implications as it suggests that

combination of radiotherapy with MET inhibition can radiosensitize cancer cells. These findings are particularly relevant for clinical situations where irradiation doses are limited by radiotoxicity, as in the case of glioblastoma (59). MET inhibition might increase the success of total brain irradiation with lower doses of IR. This strategy is consistent with the results obtained with administration of ribozymes targeting *MET*in glioblastoma cells (60). Although ribozymes are far from being suitable for therapeutic application, small-molecule kinase inhibitors (15), as well as anti-MET antibodies (61) are already available for clinical trials, and could be immediately tested in association with radiotherapy.

Our study has limitations that must be addressed in future work to fully explore the potential applications of MET inhibitors in human therapy. Although we showed that IR-induced MET expression contributes to radioresistance, it remains to be elucidated whether and under which circumstances radiotherapy promotes MET-mediated cancer invasiveness in patients. Another relevant issue that requires further investigation is whether, as observed in vitro and in vivo, the irradiated tumor microenvironment secretes factors such as TNF-± and HGF, which, by paracrine mechanisms, upregulate and activate MET within the tumor and adjacent tissues, thus propagating a bystander effect (62) and enforcing radioresistance. Finally, it would be crucial to investigate whether the cancer stem cell subpopulation, identified in human tumors such as glioblastoma, which is known to be radioresistant (7), can be eradicated by combining radiotherapy with MET inhibitors.

Funding

Italian Association for Cancer Research (AIRC Investigator Grants and “2010 Special Program Molecular Clinical Oncology 5xMille, 9970”), Regione Piemonte (Piattaforme Biotecnologiche, project PI-STEM), European Union Framework Programs (FP7/2007–2011 201279 and 201640), Compagnia di S.Paolo, CRT Foundation, and Italian Ministry of University and Research (MIUR-PRIN).

Footnotes

Funding agencies were not involved in conception and design of the study, or in any phase of data collection, analysis and interpretation, or in manuscript writing and submission. T. Perera is an employee of Janssen Pharmaceutica NV, which formulated and provided the MET inhibitor JNJ-38877605 and was not involved in collection, analysis, and interpretation of results concerning the inhibitor.

We thank Barbara Baiotto for computation of irradiation parameters; Viola Bigatto for help with experiments; Livio Trusolino, Selma Pennacchietti, Andrea Bertotti, and Cristina Basilico for critical discussion; Eleonora Urbano, Raffaella Albano, and Laura Palmas for technical assistance; Antonino Ferraro for help with computer graphics; and Antonella Cignetto and Michela Bruno for secretarial assistance.

References

1. Bernier J, Hall EJ, Giaccia A . Radiation oncology: a century of achievements. Nat Rev Cancer. 2004;4(9):737-747.

2. Suit HD. Local control and patient survival. Int J Radiat Oncol Biol Phys.1992;23(3):653-660.

3. Kaplan HS, Murphy ED. The effect of local Roentgen irradiation on the biological behaviour of a transplantable mouse carcinoma. Increased frequency of pulmonary metastasis. J Natl Cancer Inst. 1949;9(5–6):407-413.

4. von Essen CF. Radiation enhancement of metastasis: a review. Clin Exp Metastasis. 1991;9(2):77-104.

5. Lovey J, Fazekas K, Ladanyi A, Nemeth G, Timar J. Low-dose irradiation and short-exposure suboptimal-dose paclitaxel adversely modulate metastatic potential of squamous carcinoma cells. Strahlenther Onkol. 2003;179(12):812-818.

6. Hegedus B, Zach J, Czirok A, Lovey J, Vicsek T. Irradiation and taxol treatment result in non-monotonous, dose-dependent changes in the motility of glioblastoma cells. J Neurooncol. 2004;67(1–2):147-157.

7. Bao S, Wu Q, McLendon RE, et al. Glioma stem cells promote radioresistance by preferential activation of the DNA damage response. Nature. 2006;444(7120):756-760.

8. Phillips TM, McBride WH, Pajonk F. The response of CD24(-/low)/CD44+ breast cancer-initiating cells to radiation. J Natl Cancer Inst. 2006;98(24):1777-1785.

9. Baumann M, Krause M, Hill R. Exploring the role of cancer stem cells in radioresistance. Nat Rev Cancer. 2008;8(7):545-554.

10. Barcellos-Hoff MH, Park C, Wright EG. Radiation and the microenvironment—tumorigenesis and therapy. Nat Rev Cancer. 2005;5(11):867-875.

11. Shiloh Y. ATM and related protein kinases: safeguarding genome integrity. Nat Rev Cancer. 2003;3(3):155-168.

12. Thiery JP, Sleeman JP. Complex networks orchestrate epithelial-mesenchymal transitions. Nat Rev Mol Cell Biol. 2006;7(2):131-142.

13. Trusolino L, Comoglio PM. Scatter-factor and semaphorin receptors: cell signalling for invasive growth. Nat Rev Cancer. 2002;2(4):289-300.

14. Boccaccio C, Comoglio PM. Invasive growth: a MET-driven genetic programme for cancer and stem cells. Nat Rev Cancer. 2006;6(8):637-645.

15. Comoglio PM, Giordano S, Trusolino L. Drug development of MET inhibitors: targeting oncogene addiction and expedience. Nat Rev Drug Discov. 2008;7(6):504-516.

16. Scheel C, Onder T, Karnoub A, Weinberg RA. Adaptation versus selection: the origins of metastatic behavior. Cancer Res. 2007;67(24):11476-11479.

17. Thiery JP, Acloque H, Huang RY, Nieto MA. Epithelial-mesenchymal transitions in development and disease. Cell. 2009;139(5):871-890.

18. Qian LW, Mizumoto K, Inadome N, et al. Radiation stimulates HGF receptor/c-Met expression that leads to amplifying cellular response to HGF stimulation via upregulated receptor tyrosine phosphorylation and MAP kinase activity in pancreatic cancer cells. Int J Cancer. 2003;104(5):542-549.

19. Schweigerer L, Rave-Frank M, Schmidberger H, Hecht M. Sublethal irradiation promotes invasiveness of neuroblastoma cells. Biochem Biophys Res Commun.2005;330(3):982-988.

20. Prat M, Narsimhan RP, Crepaldi T, Nicotra MR, Natali PG, Comoglio PM. The receptor encoded by the human c-MET oncogene is expressed in hepatocytes, epithelial cells and solid tumors. Int J Cancer. 1991;49(3):323-328.

21. Naldini L, Vigna E, Ferracini R, et al. The tyrosine kinase encoded by the MET proto-oncogene is activated by autophosphorylation. Mol Cell Biol. 1991;11(4):1793-1803.

22. Michieli P, Basilico C, Pennacchietti S, et al. Mutant Met-mediated transformation is ligand-dependent and can be inhibited by HGF antagonists. Oncogene.1999;18(37):5221-5231.

23. Gambarotta G, Boccaccio C, Giordano S, Ando M, Stella MC, Comoglio PM. Ets up-regulates MET transcription. Oncogene. 1996;13(9):1911-1917.

24. Franken NA, Rodermond HM, Stap J, Haveman J, van BC. Clonogenic assay of cells in vitro. Nat Protoc. 2006;1(5):2315-2319.

25. Boccaccio C, Gaudino G, Gambarotta G, Galimi F, Comoglio PM. Hepatocyte growth factor (HGF) receptor expression is inducible and is part of the delayed-early response to HGF. J Biol Chem. 1994;269(17):12846-12851.

26. Pennacchietti S, Michieli P, Galluzzo M, Mazzone M, Giordano S, Comoglio PM.Hypoxia promotes invasive growth by transcriptional activation of the met protooncogene. Cancer Cell. 2003;3(4):347-361.

27. Giordano S, Ponzetto C, Di Renzo MF, Cooper CS, Comoglio PM. Tyrosine kinase receptor indistinguishable from the c-met protein. Nature. 1989;339(6220):155-156.

28. Gu H, Neel BG. The 'gab' in signal transduction. Trends Cell Biol.2003;13(3):122-130.

29. Christensen JG, Schreck R, Burrows J, et al. A selective small molecule inhibitor of c-Met kinase inhibits c-Met-dependent phenotypes in vitro and exhibits cytoreductive antitumor activity in vivo. Cancer Res. 2003;63(21):7345-7355.

30. Schmidt-Ullrich RK, Contessa JN, Lammering G, Amorino G, Lin PS. ERBB receptor tyrosine kinases and cellular radiation responses. Oncogene.2003;22(37):5855-5865.

31. Criswell T, Leskov K, Miyamoto S, Luo G, Boothman DA. Transcription factors activated in mammalian cells after clinically relevant doses of ionizing radiation.Oncogene. 2003;22(37):5813-5827.

32. Hayden MS, Ghosh S. Shared principles in NF-kappaB signaling. Cell.2008;132(3):344-362.

33. Gilmore TD. Rel/NF-kB Transcription Factors. 2008. www.NF-kB.org. Accessed January 11, 2011.

34. Nowak DE, Tian B, Jamaluddin M, et al. RelA Ser276 phosphorylation is required for activation of a subset of NF-kappaB-dependent genes by recruiting cyclin-dependent kinase 9/cyclin T1 complexes. Mol Cell Biol. 2008;28(11):3623-3638.

35. Hayden MS, Ghosh S. Signaling to NF-kappaB. Genes Dev. 2004;18(18):2195-2224.

36. Dai JY, DeFrances MC, Zou C, Johnson CJ, Zarnegar R. The Met protooncogene is a transcriptional target of NF kappaB: implications for cell survival. J Cell Biochem.2009;107(6):1222-1236.

37. Karin M, Cao Y, Greten FR, Li ZW. NF-kappaB in cancer: from innocent bystander to major culprit. Nat Rev Cancer. 2002;2(4):301-310.

38. Pouyssegur J, Mechta-Grigoriou F. Redox regulation of the hypoxia-inducible factor. Biol Chem. 2006;387(10–11):1337-1346.

39. Leach JK, Van TG, Lin PS, Schmidt-Ullrich R, Mikkelsen RB. Ionizing radiation-induced, mitochondria-dependent generation of reactive oxygen/nitrogen. Cancer Res.2001;61(10):3894-3901.

40. Rius J, Guma M, Schachtrup C, et al. NF-kappaB links innate immunity to the hypoxic response through transcriptional regulation of HIF-1alpha. Nature.2008;453(7196):807-811.

41. The Wellcome Trust Sanger Institute. www.sanger.ac.uk. 2008. Accessed January 11, 2011.

42. Bullock AN, Fersht AR. Rescuing the function of mutant p53. Nat Rev Cancer.2001;1(1):68-76.

43. Seol DW, Chen Q, Smith ML, Zarnegar R. Regulation of the c-met proto-oncogene promoter by p53. J Biol Chem. 1999;274(6):3565-3572.

44. Janssens S, Tschopp J. Signals from within: the DNA-damage-induced NF-kappaB response. Cell Death Differ. 2006;13(5):773-784.

45. Crescenzi E, Palumbo G, de BJ, Brady HJ. Ataxia telangiectasia mutated and p21CIP1 modulate cell survival of drug-induced senescent tumor cells: implications for chemotherapy. Clin Cancer Res. 2008;14(6):1877-1887.

46. Stoker M, Gherardi E, Perryman M, Gray J. Scatter factor is a fibroblast-derived modulator of epithelial cell mobility. Nature. 1987;327(6119):239-242.

47. Albini A, Benelli R. The chemoinvasion assay: a method to assess tumor and endothelial cell invasion and its modulation. Nat Protoc. 2007;2(3):504-511.

48. Trusolino L, Cavassa S, Angelini P, et al. HGF/scatter factor selectively promotes cell invasion by increasing integrin avidity. FASEB J. 2000;14(11):1629-1640.

49. Montesano R, Matsumoto K, Nakamura T, Orci L. Identification of a fibroblast-derived epithelial morphogen as hepatocyte growth factor. Cell. 1991;67(5):901-908.

50. Montesano R, Soulie P, Eble JA, Carrozzino F. Tumour necrosis factor alpha confers an invasive, transformed phenotype on mammary epithelial cells. J Cell Sci.2005;118(pt 15):3487-3500.

51. Bertotti A, Comoglio PM. Tyrosine kinase signal specificity: lessons from the HGF receptor. Trends Biochem Sci. 2003;28(10):527-533.

52. Perera T, Lavrijssen T, Janssens B. JNJ-38877605: a selective Met kinase inhibitor inducing regression of Met driven tumor models. Presented at the 99th AACR Annual Meeting; 2008 April 12–16; San Diego (CA): Abstract 4837.

53. Eder JP, Vande Woude GF, Boerner SA, LoRusso PM. Novel therapeutic inhibitors of the c-Met signaling pathway in cancer. Clin Cancer Res. 2009;15(7):2207-2214.
Abstract/FREE Full Text

54. Karin M, Lin A. NF-kappaB at the crossroads of life and death. Nat Immunol.2002;3(3):221-227.

55. Karin M. Nuclear factor-kappaB in cancer development and progression.
Nature. 2006;441(7092): 431-436.

56. Ahmed KM, Li JJ. NF-kappa B-mediated adaptive resistance to ionizing radiation. Free Radic Biol Med. 2008;44(1):1-13.

57. Stone HB, Coleman CN, Anscher MS, McBride WH. Effects of radiation on normal tissue: consequences and mechanisms. Lancet Oncol. 2003;4(9):529-536.

58. Sonnenberg E, Meyer D, Weidner KM, Birchmeier C. Scatter factor/hepatocyte growth factor and its receptor, the c-met tyrosine kinase, can mediate a signal exchange between mesenchyme and epithelia during mouse development. J Cell Biol.1993;123(1):223-235.

59. Brandsma D, Stalpers L, Taal W, Sminia P, van den Bent MJ. Clinical features, mechanisms, and management of pseudoprogression in malignant gliomas. Lancet Oncol. 2008;9(5):453-461.

60. Lal B, Xia S, Abounader R, Laterra J. Targeting the c-Met pathway potentiates glioblastoma responses to gamma-radiation. Clin Cancer Res. 2005;11(12):4479-4486.
Abstract/FREE Full Text

61. Vigna E, Pacchiana G, Mazzone M, et al. 'Active' cancer immunotherapy by anti-Met antibody gene transfer. Cancer Res. 2008;68(22):9176-9183.

62. Prise KM, O'Sullivan JM. Radiation-induced bystander signalling in cancer therapy. Nat Rev Cancer. 2009;9(5):351-360.

Supplementary methods

Chromatin immunoprecipitation (ChIP)

4×10^7 cells were used for 10 immunoprecipitations either for irradiated or control cells. After irradiation (10 Gy), cells were fixed in 1% formaldehyde for 15 minutes at room temperature, and reaction was stopped with glycine (0.125 M). Fixed cells were washed, collected in ice cold PBS supplemented with a cocktail of protease inhibitors and centrifuged. The cytoplasmic fraction was extracted as above and discarded, and nuclei were pelletted and resuspended in 1 ml of SDS-Lysis Buffer (1% SDS, 1 mM EDTA, 50 mM Tris-HCl pH 8, and a cocktail of protease inhibitors). Nuclei were then disrupted by sonication, yielding DNA fragments with a bulk size of 400-1000 bp. Cell debris were cleared by centrifugation at 17000 g for 10 minutes at 4°C. The supernatants containing the chromatin preparation were diluted with Dilution Buffer 10× (0.01% SDS, 1.1% Triton X-100, 1.2 mM EDTA, 16.7 mM Tris-HCl pH 8, 167 mM NaCl). Chromatin was then pre-cleared for 1 hour at 4°C by adding protein G-sepharose (Amersham, 50% gel slurry supplemented with 0.2 mg/mL of salmon sperm DNA, 0.1% BSA and 0.05% NaN_3). Beads were pelleted by a brief centrifugation at 1500 g at 4°C and supernatants were collected. 3% of chromatin preparation was used as Input for ChIP normalisation. ChIP was performed overnight at 4°C with 4 μg of antibodies (rabbit polyclonal anti-p65/RelA, Santa Cruz; total mouse IgG, Chemicon), followed by incubation with 50 μL of protein G-sepharose beads for 3 hours. Beads were washed sequentially on a rotating platform at 4°C with the following solutions (10 minutes/each): twice with Low-Salt Buffer (0.1% SDS, 1% Triton X-100, 2 mM EDTA, 20 mM Tris-HCl pH 8, 150 mM NaCl), twice with High-Salt Buffer (0.1% SDS, 1% Triton X-100, 2 mM EDTA, 20 mM

Tris-HCl pH 8, 500 mM NaCl), once with LiCl Buffer (0.25 M LiCl, 1% Deoxycholic Acid, 0.5% NP-40, 1 mM EDTA, 10 mM Tris-HCl pH 8), and twice with TE (10 mM Tris-HCl pH 8, 1 mM EDTA). ChIPs were eluted twice in EB (1% SDS, 0.1 M $NaHCO_3$) and kept overnight at 65°C to reverse formaldehyde cross-linking. Treatment with RNase (50 μg/mL, 37°C for 30 minutes) and Proteinase-K (500 μg/mL, 45°C for 2 hours) were performed. Each sample was purified by phenol/chloroform extraction and finally resuspended in 40 μL of sterile water. 2 μL of each sample were used as template for Real-Time PCR with SYBR GREEN PCR Master Mix (Applied Biosystems) on ABI PRISM 7900HT sequence detection system (Applied Biosystems).

Primers used were as follows: NFKBIA [sense, 5'GAACCCCAGCTCAGGGTTTAG-3'; antisense, 5'GGGAATTTCCAAGCCAGTCA-3']; -κB1 (MET) [sense, 5'AGGCCCAGTGCCTTATTACCA-3'; antisense, 5'GCGGCCTGACTGGAGATTT-3']; –κB1 (MET) [sense, 5'GGGACTCAGTTTCTTTACCTGCAA-3'; antisense, 5'GGGACTCAGTTTCTTTACCTGCAA-3'].

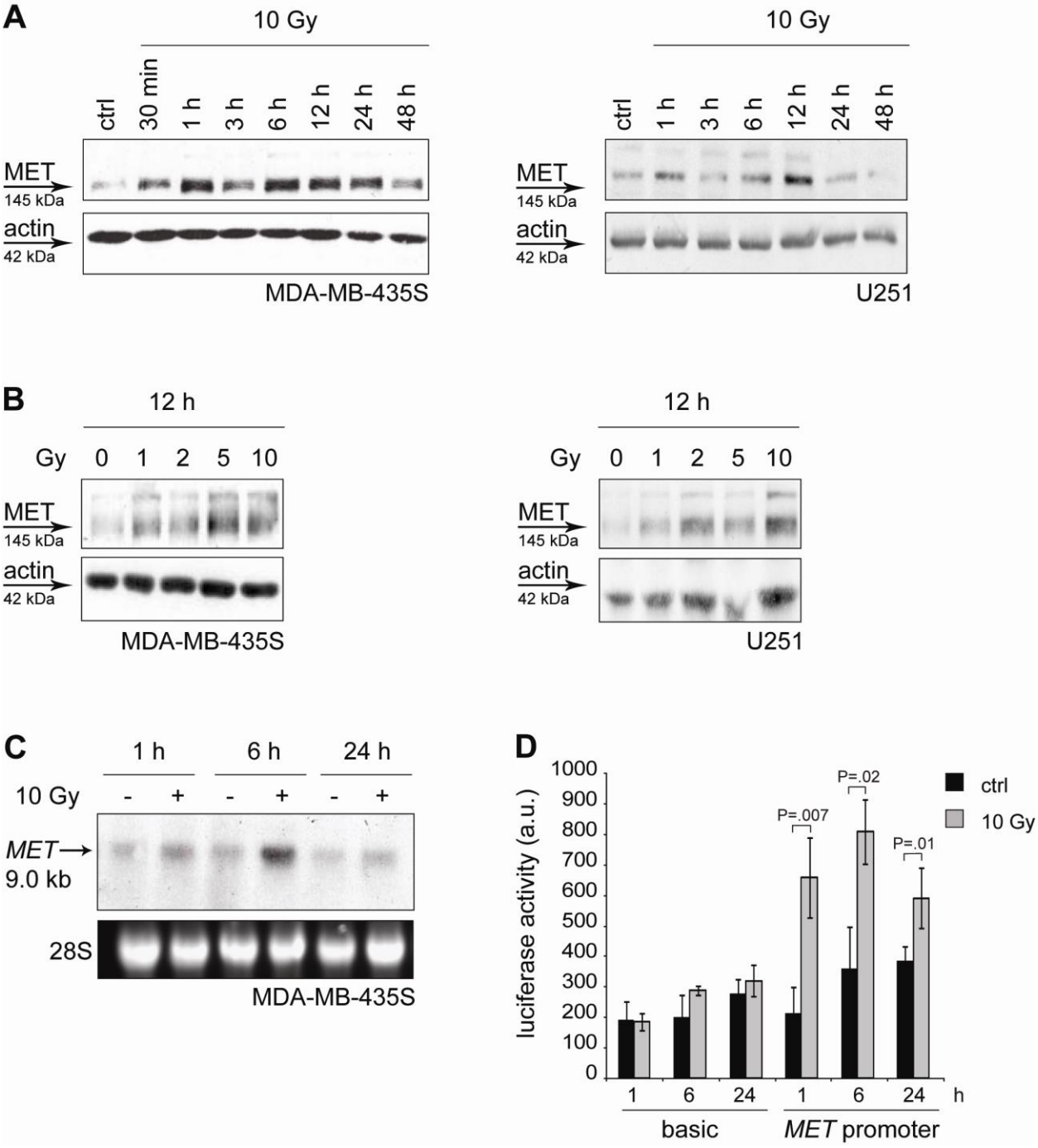

Supplementary Figure 1. Effect of ionizing radiation (IR) on MET transcription. **A**) Time course of MET protein expression in MDA-MB-435 cells (left) or U251 cells (right) after irradiation. Cell lysates were analyzed at the indicated time points after irradiation (10 Gy) by immunoblotting with anti-MET antibodies. The control lane (ctrl) shows MET expression at time zero. Blots were also probed with anti-actin antibodies as a control of protein loading. **B**) Dose-response of MET protein induction after irradiation. Lysates from MDA-MB-435S cells (left) or U251 cells (right) were analyzed at 12 hours after irradiation (from 0 to 10 Gy) by

immunoblotting with anti-MET antibodies. Blots were probed also with anti-actin antibodies as a control of protein loading. **C**) Time course of MET mRNA induction in MDA-MB-435S after irradiation. RNA was extracted 1, 6, or 24 hours after irradiation (10 Gy) and examined by Northern blotting using a probe to the entire coding sequence of MET. Ribosomal subunit 28S was measured as control of RNA loading. Similar results were obtained with U251 cells (data not shown). **D**) *MET* promoter activity in irradiated MDA-MB-435S cells. Plasmids expressing the luciferase gene under control of the *MET* promoter were transfected and, after 48 hours, cells were irradiated (10 Gy). Then, luciferase activity was measured at 1, 6, or 24 hours and normalized for protein expression. (ctrl = non-irradiated cells; basic = cells transfected with a plasmid containing a promoterless luciferase gene and treated as above). The means of six samples from two independent experiments and their 95% confidence intervals are shown. (P values are from two-sided paired t-tests; a.u. = arbitrary units).

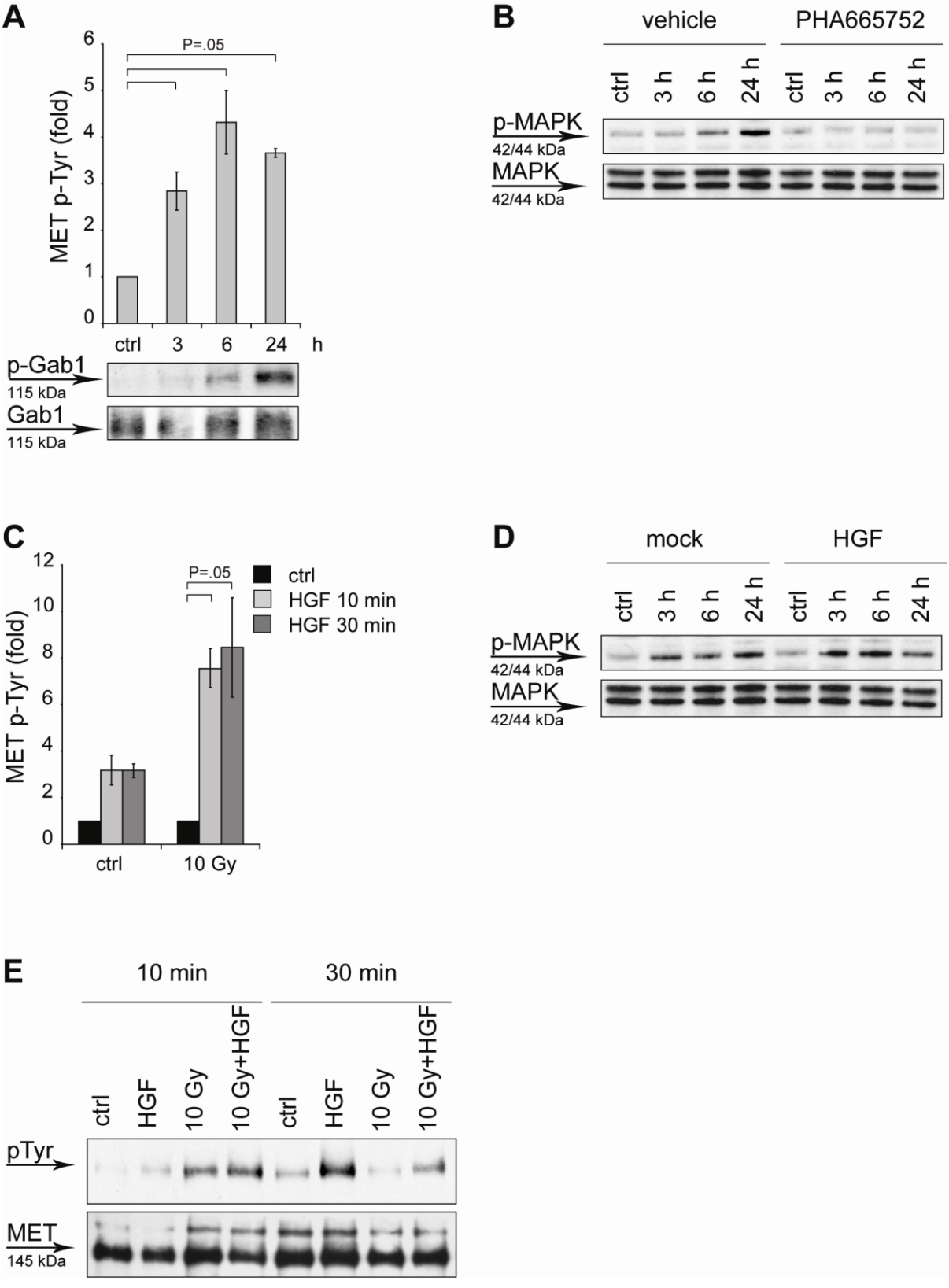
A
MET p-Tyr (fold)
P=.05
ctrl
3
6
24
h
p-Gab1
115 kDa
Gab1
115 kDa
B
vehicle
PHA665752
ctrl
3 h
6 h
24 h
p-MAPK
42/44 kDa
MAPK
42/44 kDa
C
MET p-Tyr (fold)
P=.05
ctrl
HGF 10 min
HGF 30 min
ctrl
10 Gy
D
mock
HGF
ctrl
3 h
6 h
24 h
p-MAPK
42/44 kDa
MAPK
42/44 kDa
E
10 min
30 min
ctrl
HGF
10 Gy
10 Gy+HGF
pTyr
MET
145 kDa

Supplementary Figure 2. Effect of ionizing radiation (IR) on MET signaling. **A**) Tyrosine phosphorylation of MET and Gab1 after irradiation. Cell lysates from U251 cells were immunoprecipitated with anti-MET antibodies 3, 6, or 24 hours after irradiation (10 Gy) and analyzed by immunoblotting with mouse monoclonal anti-phosphotyrosine antibodies. The same blots were stripped and reprobed with anti-Met antibodies. **Upper panel**: the amount of MET tyrosine phosphorylation was quantified and normalized against the amount of MET protein detected in immunoblots. The trend of MET phosphorylation, represented as the ratio (MET pTyr fold) of normalized MET phosphorylation in irradiated vs non-irradiated cells, was graphed as the mean of two independent experiments with 95% confidence intervals. MET phosphorylation levels in non-irradiated cells (ctrl) were arbitrarily set to 1. *P* values are from two-sided paired t-tests. **Middle panel**: on blots of anti-MET immunoprecipitates, an anti-phosphotyrosine antibody recognized a phosphoprotein with a molecular weight (115 kDa) corresponding to Gab1 (P-Gab1). **Lower panel**: the above blots were stripped and reprobed with rabbit polyclonal anti-Gab1 antibodies, confirming the identity of the protein coprecipitated with MET (Gab1). **B**) MET-dependent activation of mitogen-activated protein kinases (MAPK) after irradiation. U251 cells were treated with the MET kinase inhibitor PHA665752 (500 nM) or DMSO (vehicle), and analyzed 3, 6, or 24 hours after irradiation (10 Gy) by immunoblotting with rabbit polyclonal antibodies recognizing the serine-phosphorylated form of p42/p44 MAPK (p-MAPK). The control lane (ctrl) shows MAPK phosphorylation at time zero. Blots were stripped and reprobed with rabbit polyclonal anti-MAPK antibodies to show equal protein amounts. **C**) Tyrosine phosphorylation of MET after irradiation and HGF stimulation. Twelve hours after irradiation (10 Gy), U251 cells were treated with HGF (50 ng/mL) for 10 or 30 minutes. Lysates were immunoprecipitated with anti-MET antibodies and analyzed by immunoblotting with anti-phosphotyrosine antibodies. Blots were stripped and reprobed with anti-MET antibodies. Nonirradiated cells were immunoprecipitated with anti-MET antibodies as a control (ctrl). The amount of MET tyrosine phosphorylation was quantified and normalized against the amount of MET protein detected on immunoblots. The ratio (MET pTyr fold) of normalized MET phosphorylation in HGF-stimulated vs mock-stimulated cells was shown as the mean of two independent experiments with 95% confidence intervals. MET phosphorylation levels in mock-stimulated cells (ctrl) were arbitrarily set to 1. *P* values were from two-sided paired t-tests. **D)** Activation of MAP kinases in irradiated and HGF-stimulated cells. U251 cells were stimulated with HGF (50 ng/mL) immediately before irradiation (10 Gy), and analyzed 3, 6, or 24 hours after irradiation by immunoblotting with antibodies recognizing the serine phosphorylated form of p42/p44 MAPK or total MAPK as in (B). **E)** MET phosphorylation at early time-points after irradiation. MDA-MB-231 cells were irradiated (10 Gy) and/or treated with HGF (50 ng/mL). At 10 or 30 minutes after treatment, lysates were immunoprecipitated with anti-MET antibodies and analyzed by immunoblotting with anti-phospho-tyrosine antibodies (pTyr). The control lane (ctrl) shows the level of MET phosphorylation in non-irradiated U251 cells. The same blots were stripped and reprobed with anti-MET antibodies as a control of equal protein immunoprecipitation.

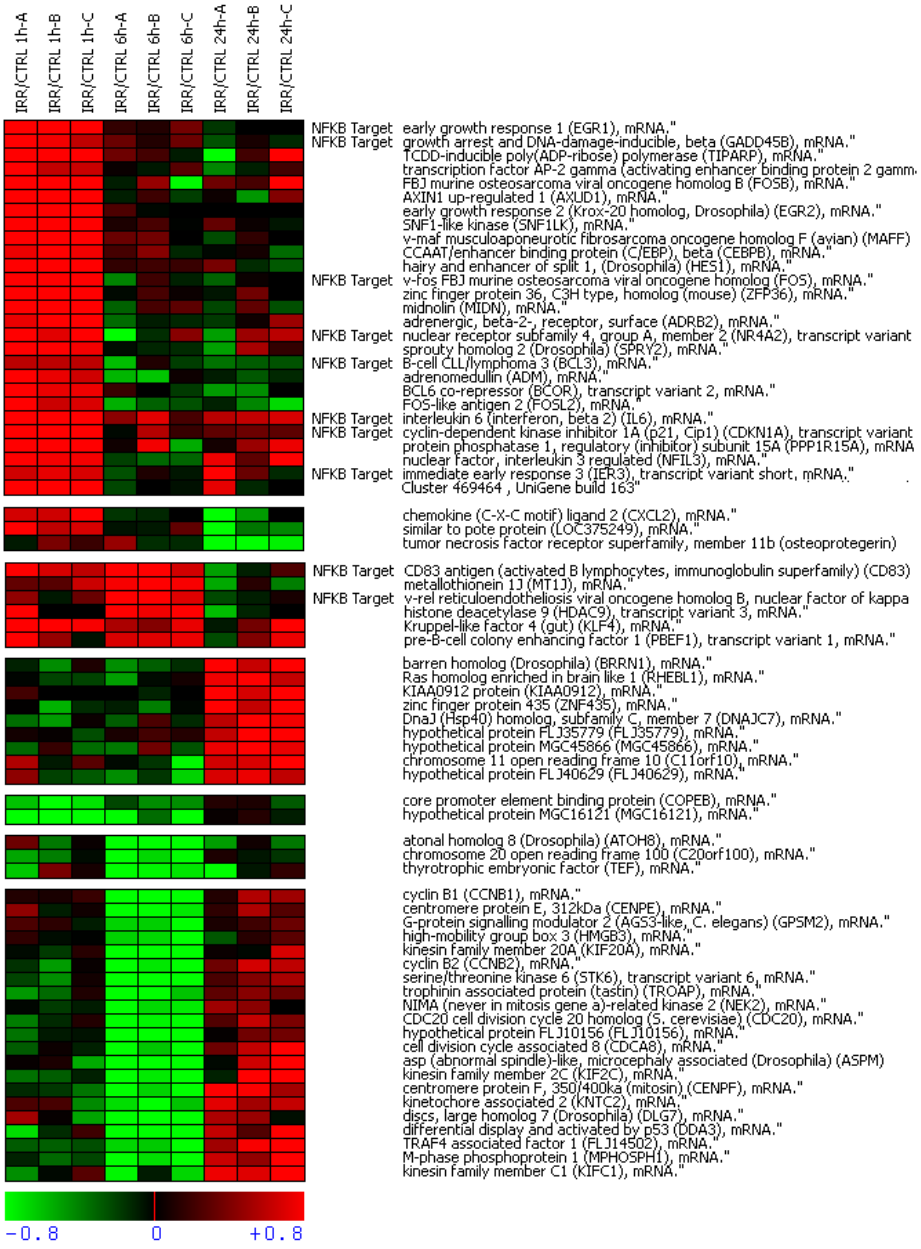

Supplementary Figure 3. Gene expression profiling in irradiated cells. Microarrays were used to evaluate the transcriptional response of MDA-MB-231 cells to ionizing radiation (IR). Subconfluent cells were serum-starved for 48 hours and irradiated (10 Gy). At 1, 6, or 24 hours after irradiation, biotin-labeled complementary RNAs were obtained from 10 μg of total RNA samples, amplified according to Illumina TotalPrep RNA Amplification Kit (Ambion Inc. Austin, TX), and hybridized with human WG-6 Beadarrays (Illumina, Muenchen, Germany). Raw data were rank-invariant normalized and filtered for statistical significance detection using the BeadStudio software (Illumina). Microsoft Excel was used for identification of regulated genes and hypergeometric analysis of NF-κB targets (Supplementary Table 1). For each time

point, regulated genes were defined as those displaying at least a 1.5 fold-change in each of the triplicate comparisons with non-irradiated cells. The list of NF-κB target genes, obtained from www.NF-kB.org, was mapped on the dataset. The fraction of NF-κB targets in the IR-responsive gene set was compared with the fraction of NF-κB targets in the whole dataset by hypergeometric distribution analysis. The diagram above shows genes for which there are statistically significant differences in expression ($P \leq .05$). Columns show $\log_2$ ratio of gene expression of irradiated (IRR) vs non-irradiated cells (CTRL) at three different time-points (1, 6, 24 hours), in three independent experiments (A-C). One hour after irradiation, NF-κB target genes (www.NF-kB.org) were enriched ~20 times more than expected (hypergeometric *P*-value $<10^{-9}$). For the complete list of genes modulated by IR, see Supplementary Table 1.

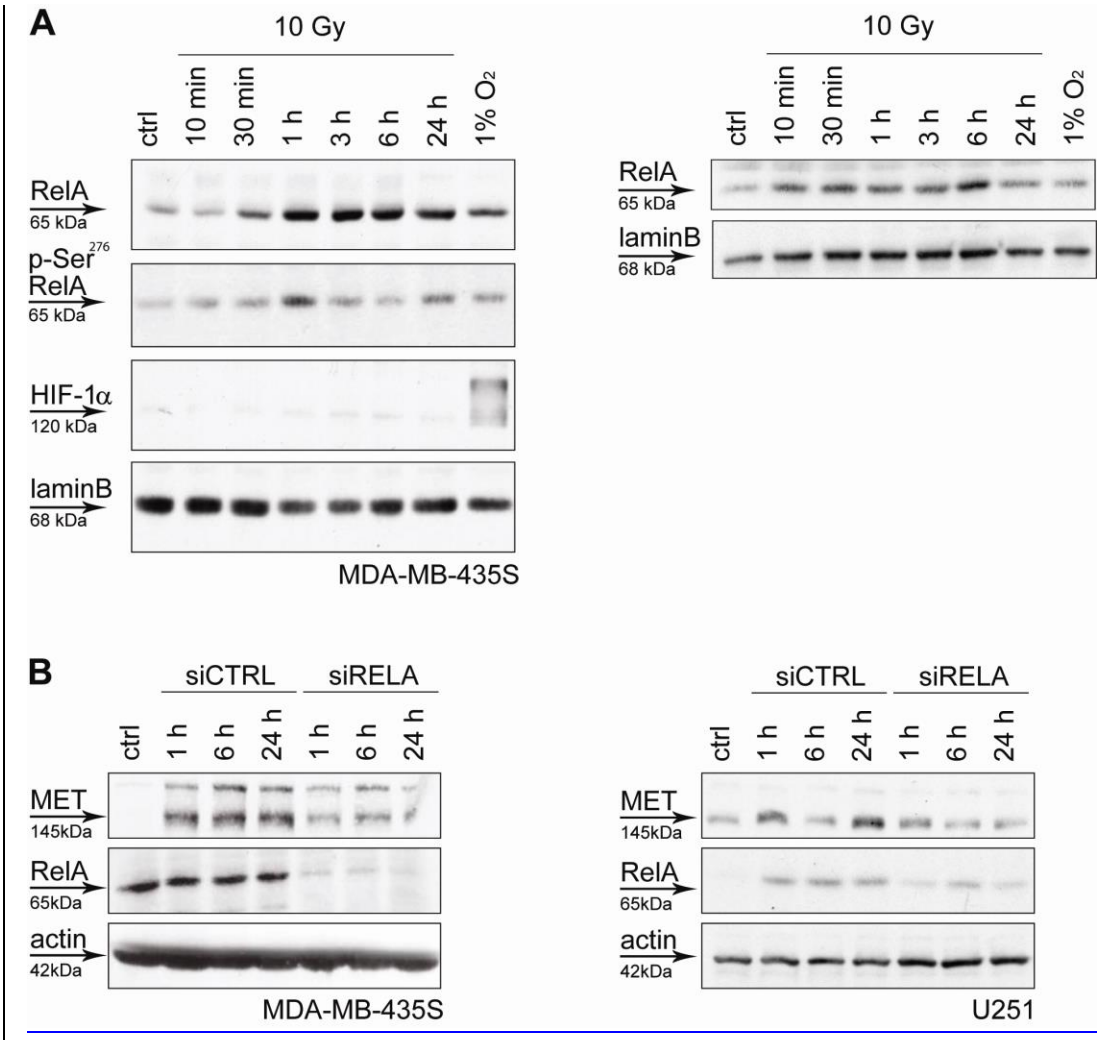

Supplementary Figure 4. Role of NF-κB in MET transcription induced by ionizing radiation IR. **A**) Accumulation of p65/RelA in cell nuclei after irradiation. Nuclear extracts from MDA-MB-435S cells (left) or U251 (right) were immunoblotted with specific antibodies to show the time course of p65/RelA nuclear accumulation (RelA, mouse monoclonal anti-p65/RelA) in response to irradiation (10 Gy) or hypoxia (24 hours at 1% O_2). Non-irradiated cells at time zero served as a control (ctrl). In MDA-MB-435S (left) p65/RelA serine phosphorylation (p-Ser^{276}RelA) was analyzed with rabbit polyclonal anti-phospho-serine 276 and HIF-1α nuclear accumulation with mouse monoclonal anti-HIF-1α. Blots were stripped and reprobed with mouse monoclonal anti-lamin B as control of protein loading. **B**) RelA-dependent expression of MET after irradiation. MDA-MB-435S cells (left) or U251 cells (right) were transfected with siRNA against p65/RelA (siRELA) or control siRNA (siCTRL) and irradiated (10 Gy). Lysates were analyzed 1, 6, or 24 hours after treatment by immunoblotting with anti-MET (MET) or anti-p65/RelA (RelA) antibodies. The control lane (ctrl) shows MET or p65/RelA expression in mock-transfected cells at time zero after irradiation. Blots were probed also with anti-actin as control of protein loading.

Supplementary Figure 5. Alignment of the human and murine *MET* promoter sequences. The human *MET* promoter (GenBank accession number AF046925) was analyzed with the TRANSFAC 7.0 software (www.gene-regulation.com) for identification of transcription factor binding sites. Two putative NF-κB binding sites (κB1 and κB2) were found. Alignment of the human and murine (Gene ID 17295) *MET* promoters showed that the κB2 site (including a sequence from -1150 to -1137 bp in the human sequence, rectangle) is highly conserved between the two species.

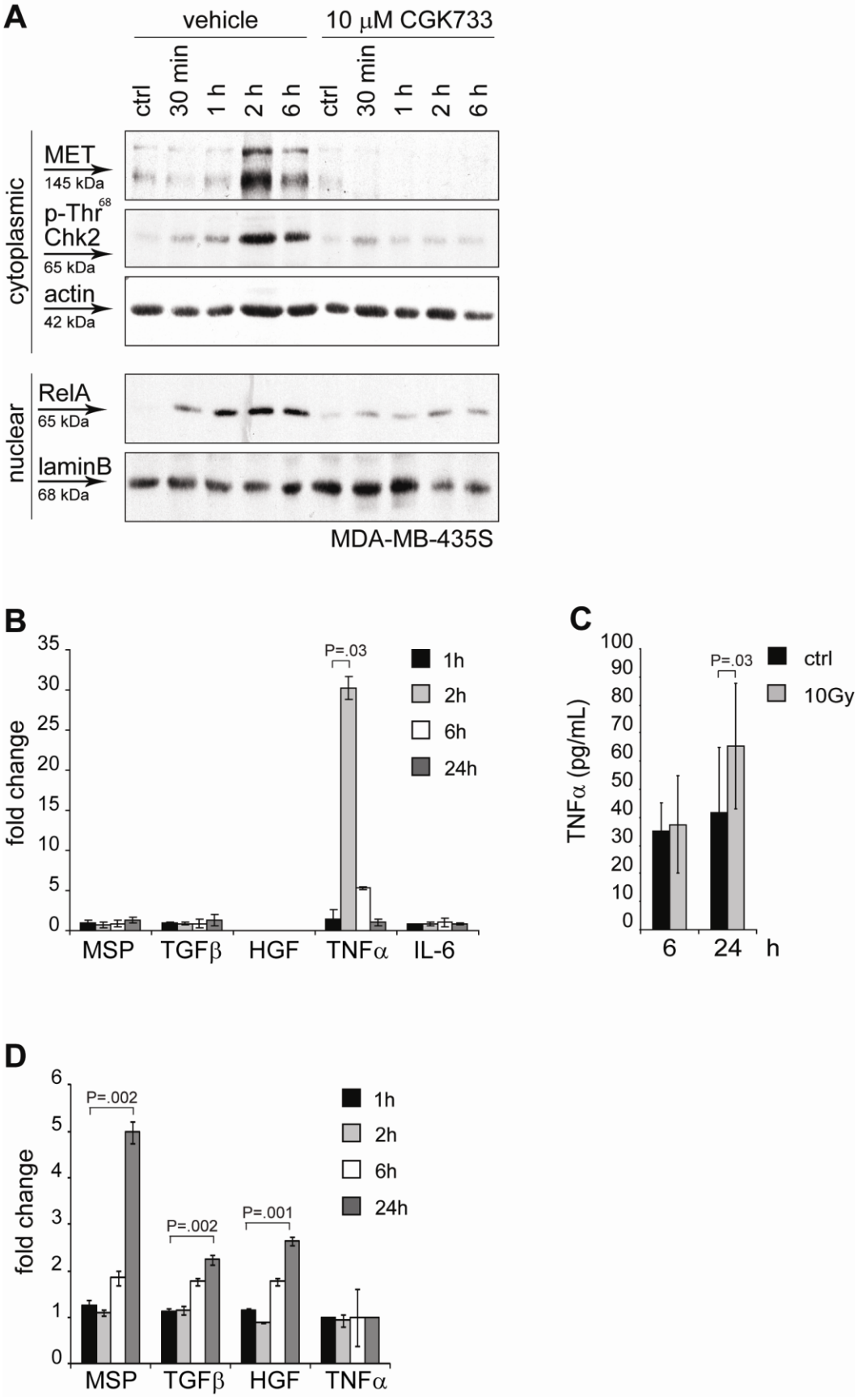
A
vehicle
10 μM CGK733
ctrl
30 min
1 h
2 h
6 h
ctrl
30 min
1 h
2 h
6 h
cytoplasmic
MET
145 kDa
p-Thr68 Chk2
65 kDa
actin
42 kDa
nuclear
RelA
65 kDa
laminB
68 kDa
MDA-MB-435S
B
fold change
P=.03
1h
2h
6h
24h
MSP
TGFβ
HGF
TNFα
IL-6
C
TNFα (pg/mL)
P=.03
ctrl
10Gy
6
24
h
D
fold change
P=.002
P=.002
P=.001
1h
2h
6h
24h
MSP
TGFβ
HGF
TNFα

Supplementary Figure 6. Role of ataxia telecangtasia mutated (ATM) kinase signaling and the tumor necrosis factor-a (TNF-α) autocrine loop in ionizing radiation (IR)-induced nuclear factor-kappa B (NF-κB) activation. **A**) Effect of the ATM kinase inhibitor, CGK733, on MET, Chk2 and p65/RelA in irradiated cells. MDA-MB-435S cells were treated with CGK733 (10 μM) or DMSO (vehicle) for 4 hours and then irradiated (10 Gy). Cytoplasmic or nuclear extracts obtained from 30 minutes to 6 hours after irradiation were analyzed by immunoblotting with specific antibodies to show MET expression, Chk2 threonine phosphorylation (p-Thr^{68} Chk2, rabbit polyclonal anti-phospho Chk2 antibodies), and p65/RelA (RelA) nuclear accumulation. Blots were stripped and reprobed with anti-actin or anti-lamin B antibodies as controls of protein loading. Non-irradiated cells at time zero served as control (ctrl). **B)** Transcription of growth factors and cytokines in irradiated MDA-MB-435S cells. RNA levels were measured by quantitative polymerase chain reaction at the indicated time-points after irradiation (10 Gy). The graph shows the fold change in RNA content in irradiated vs non-irradiated cells (means of nine samples from three independent experiments, with 95% confidence intervals; *P* values from two-sided paired t-tests). TNFα transcription was analyzed also in irradiated U251 cells, and was increased up to 28-fold 6 hours after irradiation (data not shown). **C)** TNFα secretion by irradiated MDA-MB-435S cells. Cell culture media were removed 6 or 24 hours after irradiation (10 Gy), and TNF-α concentration (pg/mL) was measured by enzyme-linked immunosorbent assays (ELISA). Non-irradiated cells served as control (ctrl). The graph shows a mean of six samples from two independent experiments, with 95% confidence intervals (*P* values from two-sided paired t-tests). **D**) Transcription of growth factors and cytokines in irradiated MRC-5 fibroblast cells. RNA levels were measured by quantitative polymerase chain reaction at the indicated time-points after irradiation (10 Gy). The graph shows the fold change in RNA content in irradiated vs non-irradiated cells (means of nine samples from three independent experiments, with 95% confidence intervals, *P* values from two-sided paired t-tests).

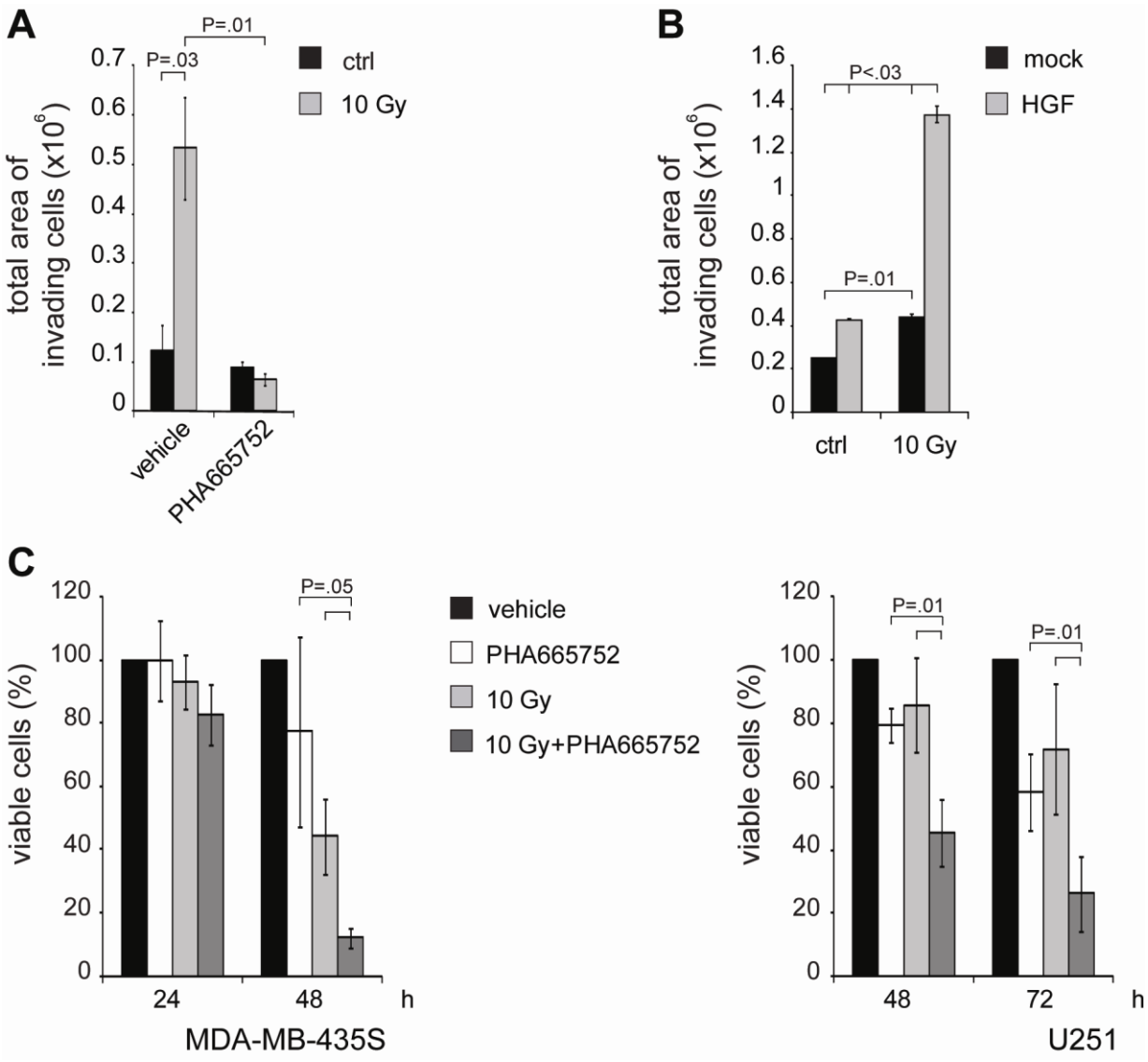

Supplementary Figure 7. Role of MET in invasive growth and decreased viability of irradiated cells. **A)** Effect of MET inhibition on IR-induced cell invasion in the transwell assay. U251 cells were seeded onto Matrigel-coated transwell filters, supplied with the MET inhibitor, PHA665752 (500 nM), or DMSO (vehicle) immediately before irradiation (10 Gy), and kept in the presence of the inhibitor during the transwell assay. After 24 hours, cells that invaded the filters were stained with crystal violet, photographs were taken at 100× magnification, and cells were counted. The graph represents the means of six samples from three independent experiments, with 95% confidence intervals (*P* values are from two-sided paired t-tests). **B**) HGF-stimulated invasiveness in the transwell assay. Experiments were performed as in (**A**) except in that U251 cells received HGF (50 ng/mL) in place of the MET inhibitor, or were mock-treated, during the transwell assay. The graph represents the means of six samples from two independent experiments with 95% confidence intervals (paired t-test). **C**) MET inhibition and viability of irradiated cells. MDA-MB-435S cells (left) or U251 cells (right) were grown to

confluence, serum-starved and irradiated (10 Gy). The MET inhibitor PHA665752 or DMSO (vehicle) were added immediately before irradiation and kept up to 48 in MDA-MB-435S cells or 72 hours in U251 cells. Cell viability was evaluated by measuring ATP production at the indicated time-points after irradiation. The graph shows means of nine samples from three independent experiments with 95% confidence intervals (*P* values from two-sided paired t-tests). Survival of non-irradiated cells kept in the presence of the vehicle was arbitrarily set to 100%.

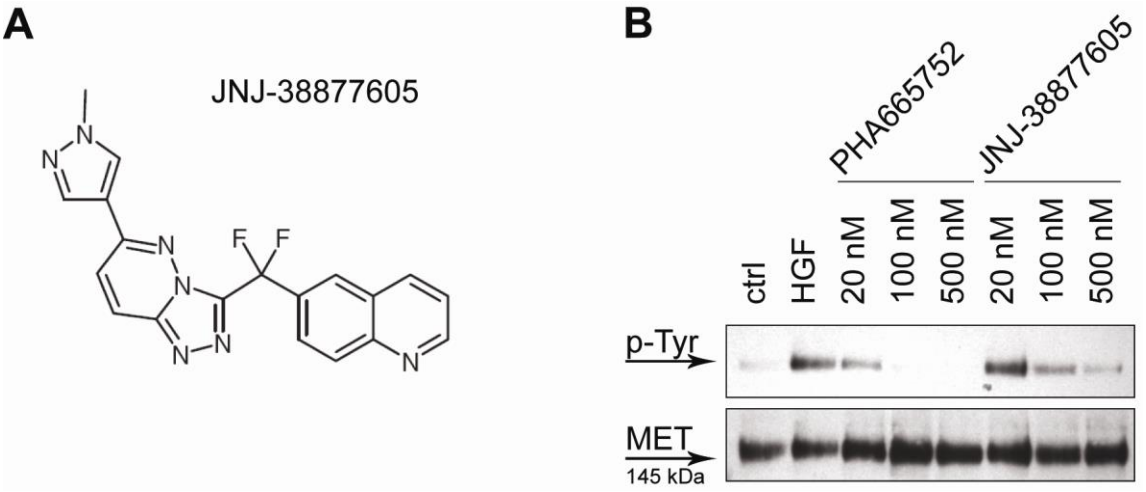

Supplementary Figure 8. MET kinase inhibition by the JNJ-38877605 compound. **A**) Chemical structure of the small-molecule Met tyrosine kinase inhibitor JNJ-38877605. Data summary (1-3): Chemical Formula: $C_{19}H_{13}F_2N_{7;}$ Molecular Weight: 377.35; Registry Number: 943540-75-8; Synthesis & NMR data are described in the patent WO2007075567; highly specific MET inhibitor (selective over more than 250 kinases tested, data not shown **[EDITOR: these data were presented in the Supplementary Table 2 that you suggested to eliminate, see Results**), ATP comptetitive; enzyme IC_{50}: 4 nM; phospho-MET IC_{50}: 50 nM; currently tested in Phase I clinical trials. **B**) Effect of JNJ-38877605 on MET tyrosine phosphorylation. MDA-MB-231 cells were stimulated with HGF (50 ng/mL) for 30 minutes (lane HGF) or pre-treated for 2 hours with increasing doses of PHA665752 (20-500 nM) or JNJ-38877605 (20-500 nM), and stimulated with HGF as above. Cell lysates were immunoprecipitated with anti-Met antibodies and analyzed by immunoblotting with anti-phospho-tyrosine antibodies (p-Tyr). The control lane (ctrl) shows mock-stimulated cells. The same blots were stripped and reprobed with anti-Met antibodies as control of protein immunoprecipitation.

References

1. Perera,T., Lavrijssen,T., and Janssens,B. 2008. JNJ-38877605: a selective Met kinase inhibitor inducing regression of Met driven tumor models. *99th AACR Annual Meeting; 2008 Apr 12-16; San Diego (CA)*. 4837 (Abstr.)

2. Comoglio, P.M., Giordano, S., and Trusolino, L. 2008. Drug development of MET inhibitors: targeting oncogene addiction and expedience. *Nat. Rev. Drug Discov.* **7**:504-516.

3. Eder, J.P., Vande Woude, G.F., Boerner, S.A., and LoRusso, P.M. 2009. Novel therapeutic inhibitors of the c-Met signaling pathway in cancer. *Clin. Cancer Res.* **15**:2207-2214.